34p

554363

NASA TR R-123

38B5

NASA TR R-123

N63-13105

NATIONAL AERONAUTICS AND SPACE ADMINISTRATION

Code 1

TECHNICAL REPORT

R-123

CALCULATIONS OF COMPRESSIBLE AVERAGE TURBULENT SKIN FRICTION

By MITCHEL H. BERTRAM

1962

For sale by the Superintendent of Documents, U.S. Government Printing Office, Washington 25, D.C. Yearly subscription, $15; foreign, $19; single copy price varies according to size ---------- Price 40 cents

TECHNICAL REPORT R-123

CALCULATIONS OF COMPRESSIBLE AVERAGE TURBULENT SKIN FRICTION

By MITCHEL H. BERTRAM

Langley Research Center
Langley Station, Hampton, Va.

CONTENTS

	Page
SUMMARY	1
INTRODUCTION	1
SYMBOLS	1
REVIEW OF EQUATIONS	2
Relation Between Reference-Temperature and Compressible Parameters	2
Evaluation of Reference Temperature	2
Incompressible Skin-Friction Relations	3
VALIDATION OF REFERENCE-TEMPERATURE APPROACH	4
Laminar Boundary Layer	4
Turbulent Boundary Layer	5
COMPUTATIONS BY REFERENCE-TEMPERATURE METHOD	6
Average Skin Friction as a Function of Mach Number	6
Average Skin Friction as Affected by Wall Temperature	8
Effect of Choice of Turbulent Incompressible Skin-Friction Law on Computations	8
Effect of Normal Shock at Leading Edge on Skin Friction	20
APPLICATION OF RESULTS TO CONE AND TAPERED PLATE	25
Average Turbulent Skin Friction for a Cone at Zero Angle of Attack	25
Average Skin Friction for a Tapered Plate	30
CONCLUDING REMARKS	30
REFERENCES	31

TECHNICAL REPORT R-123

CALCULATIONS OF COMPRESSIBLE AVERAGE TURBULENT SKIN FRICTION

By Mitchel H. Bertram

SUMMARY 13105

Calculations have been carried out for a perfect-gas flow to show the effect of a wide range of parameters on the average skin friction on a flat plate in turbulent flow by the reference-temperature method (however, to some extent laminar flow was also treated). Some of the variables were Mach number, Reynolds number, and wall and free-stream temperature level for ratios of specific heats of 7/5 and 5/3. The effect of the blunt leading edge was calculated by assuming that the turbulent boundary layer is growing in the reexpanded flow behind a normal shock at various free-stream Mach numbers. Analogous to angle of attack, the pressure level on the plate was varied over a wide range to show the effect on skin friction for the plate with sharp and blunt leading edges. Relations which allow the results to be applied to cones and wings of tapered planform were shown.

INTRODUCTION

In many computations of the characteristics of hypersonic vehicles, a knowledge of the type of boundary layer (laminar, transitional, or turbulent) that exists over the vehicle is desired. In most instances this information is not available a priori so that assumptions have to be made as to the state of the boundary layer. In general, the approach is taken that the type of boundary layer assumed is the one which gives the most conservative result.

For the laminar boundary layer, the reference-temperature or T-prime method first proposed by Rubesin and Johnson [1] (ref. 1) is a powerful approach to the calculation of boundary-layer characteristics because of its accuracy combined with relative simplicity. The reference-temperature approach has also been extended to turbulent boundary layers by Fischer and Norris (ref. 2).

The purpose of the present paper is to show the effect of wide variations in various parameters on the average skin-friction coefficient on flat plates—to some extent in laminar flow but mainly for the turbulent boundary-layer case. Monaghan's reference-temperature equations for laminar (ref. 4) and turbulent (ref. 5) boundary layers are utilized. In the development the method is validated by a comparison with more or less exact computations in the case of laminar flow and with some of the more reliable test data in the case of turbulent flow.

SYMBOLS

a, b	constants in power law for skin friction
A_1, A_2, A_3	coefficients in reference-temperature equation
B	Sutherland constant
C	coefficient in linear viscosity law
C_f	local skin-friction coefficient
C_F	average skin-friction coefficient
$k \equiv \frac{\gamma-1}{2} M_\infty^2$	
l	total length of plate
M	Mach number
n	exponent in power law for skin friction
N_{Pr}	Prandtl number
p	pressure
q	dynamic pressure
r	radius of cone
R	Reynolds number
R_θ	Reynolds number based on momentum thickness

[1] At about the same time, however, a similar modification to the incompressible formulas was proposed by Young (ref. 3).

S	reference area
T	absolute temperature
u	velocity
x	distance along plate in flow direction
γ	ratio of specific heats
λ	wing taper ratio, ratio of tip chord to root chord
μ	dynamic viscosity
ρ	density
τ	local shear stress
ω	exponent in power law for viscosity

Subscripts:

c	cone
fp	flat plate ($\lambda=1$)
i	incompressible
l	total length of plate
r	adiabatic wall
S	sharp leading edge
w	wall
x	distance along plate in flow direction
λ	tapered plate
∞	static free-stream condition
0	stagnation condition
1	pressure over plate equals undisturbed free-stream pressure
3	static conditions after expansion from conditions after normal shock

Primes denote parameters evaluated at reference-temperature conditions.

REVIEW OF EQUATIONS

RELATION BETWEEN REFERENCE-TEMPERATURE AND COMPRESSIBLE PARAMETERS

The reference-temperature method was proposed as a means of expressing the results of compressibility on skin friction in laminar flow (ref. 1) in terms of the incompressible formulas. This method, however, has also been used for turbulent flow. (See ref. 2.) In the reference-temperature approach the fluid properties are evaluated at some temperature which, to be useful, must be a single function of wall, stagnation, and stream temperature. If this temperature function exists, the skin-friction coefficient and Reynolds number with fluid properties based on this temperature are identical to those given by the incompressible skin-friction equations.

The basic relations between the compressible parameters and the same parameters evaluated at the reference temperature are as follows:

For skin-friction coefficients

$$C_F=\frac{T_\infty}{T'}C'_F \tag{1}$$

$$C_f=\frac{T_\infty}{T'}C'_f \tag{2}$$

For Reynolds number

$$R_{\infty,x}=\frac{\mu'}{\mu_\infty}\frac{T'}{T_\infty}\frac{\rho' u_\infty}{\mu'}x=\frac{\mu'}{\mu_\infty}\frac{T'}{T_\infty}R'_x \tag{3}$$

$$R_\theta=\frac{\mu'}{\mu_\infty}R'_\theta \tag{4}$$

since

$$C_F R_{\infty,x}=2R_\theta$$

and

$$C'_F R'_x=2R'_\theta$$

EVALUATION OF REFERENCE TEMPERATURE

In general, the reference-temperature equation can be written

$$T'=A_1T_w+A_2T_0+A_3T_\infty \tag{5}$$

or in terms of wall temperature and Mach number

$$T'=A_1T_w+T_\infty(1-A_1+A_2k) \tag{6}$$

For the computations presented in this paper, the coefficients suggested by Monaghan were used for both $\gamma=7/5$ and $\gamma=5/3$.

For laminar flow (ref. 4) [2]

$$\left.\begin{aligned} A_1&=1-0.468N_{Pr}^{1/3}\\ A_2&=(1-A_1-0.273\sqrt{N_{Pr}})\sqrt{N_{Pr}}\\ \frac{T_r}{T_\infty}&=1+\sqrt{N_{Pr}}k \end{aligned}\right\} \tag{7}$$

with

$$N_{Pr}=0.75;\ A_1=0.575;\ A_2=0.164$$

For turbulent flow (ref. 5)

$$\left.\begin{aligned} A_1&=0.54\\ A_2&=0.142\\ \frac{T_r}{T_\infty}&=1+0.89k \end{aligned}\right\} \tag{8}$$

[2] These values for laminar flow may be compared with those of Rubesin and Johnson (ref. 1) where $A_1=0.58$ and $A_2=0.15$ and those of Young (ref. 3) where $A_1=0.55$ and $A_2=0.16$.

where $k \equiv \frac{\gamma-1}{2} M_\infty^2$ and $A_3 = 1-(A_1+A_2)$ for both laminar and turbulent flow.

The reference-temperature ratio as a function of the Mach number parameter k for various wall-temperature ratios is shown in figure 1 for the turbulent case. The insulated-plate line in this figure represents the locus of the points for wall temperature equal to adiabatic wall temperature.

INCOMPRESSIBLE SKIN-FRICTION RELATIONS

For the laminar average skin-friction calculations the Blasius equation was used where

$$C_{F,i} = \frac{1.328}{\sqrt{R_{x,i}}} \tag{9}$$

In the turbulent case two different sets of equations were used. One was the Karman-Schoenherr formulation for average and local skin friction

$$\frac{0.242}{\sqrt{C_{F,i}}} = \log\,(C_{F,i} R_{x,i}) = \log\,(2R_{\theta,i}) \tag{10}$$

$$C_{f,i} = \frac{0.242 C_{F,i}}{0.242 + 0.8686\sqrt{C_{F,i}}} \tag{11}$$

A plot of these equations is shown in figure 2. The Karman-Schoenherr relations accurately fit the incompressible data and the reader is referred to references 6 to 8. A range of Reynolds number from about 6×10^4 to 10^9 is covered by the experimental data. The main objection to the use of the Karman-Schoenherr formula is the fact that $C_{F,i}$ is not an explicit function of $R_{x,i}$. Various interpolation formulas have been devised to remove this objection. One of the more recent suggestions is the set of equations proposed by Sivells and Payne (ref. 9) which accurately fit the Karman-Schoenherr relations in the range $10^5 < R_{x,i} < 10^9$.

$$C_{F,i} = \frac{0.088}{(\log R_{x,i} - 1.5)^2} \tag{12}$$

$$C_{f,i} = 0.088\,\frac{(\log R_{x,i} - 2.3686)}{(\log R_{x,i} - 1.5)^3} \tag{13}$$

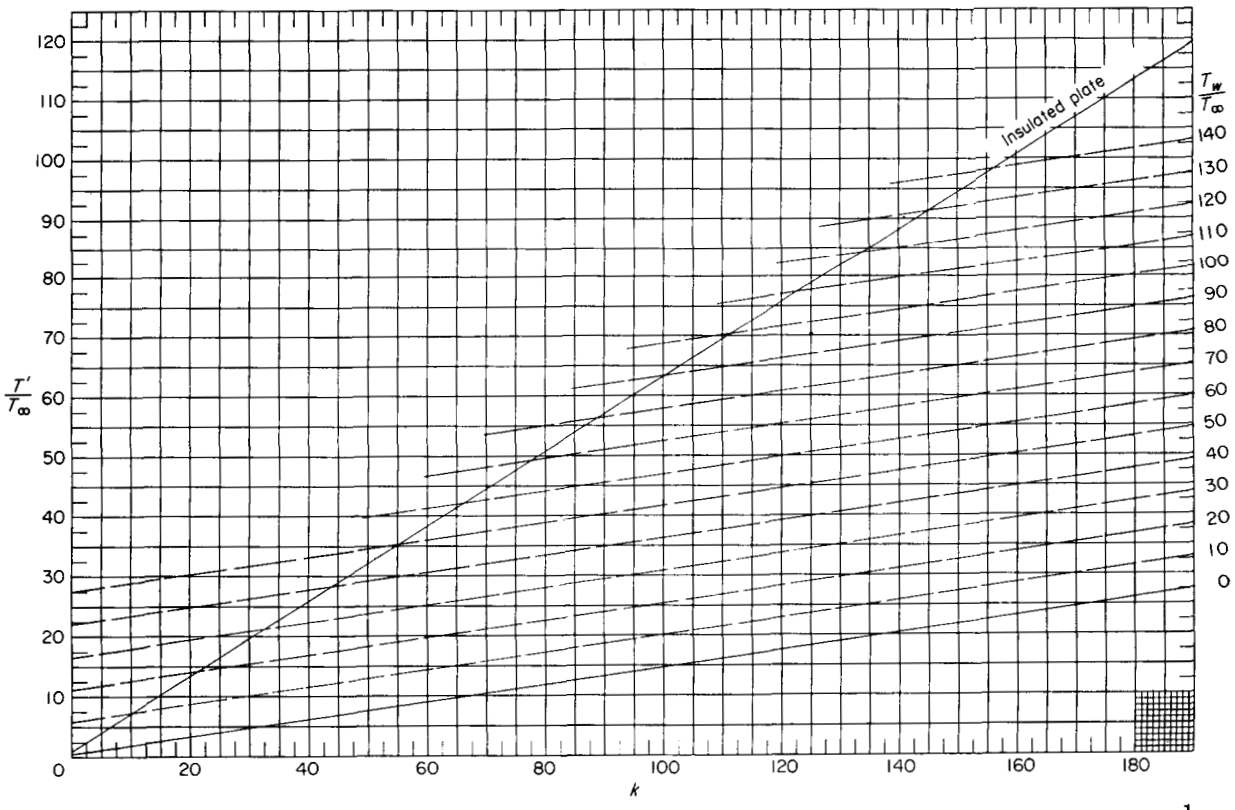

FIGURE 1.—The turbulent reference-temperature ratio as a function of the Mach number parameter k. $k \equiv \frac{\gamma-1}{2} M_\infty^2$.

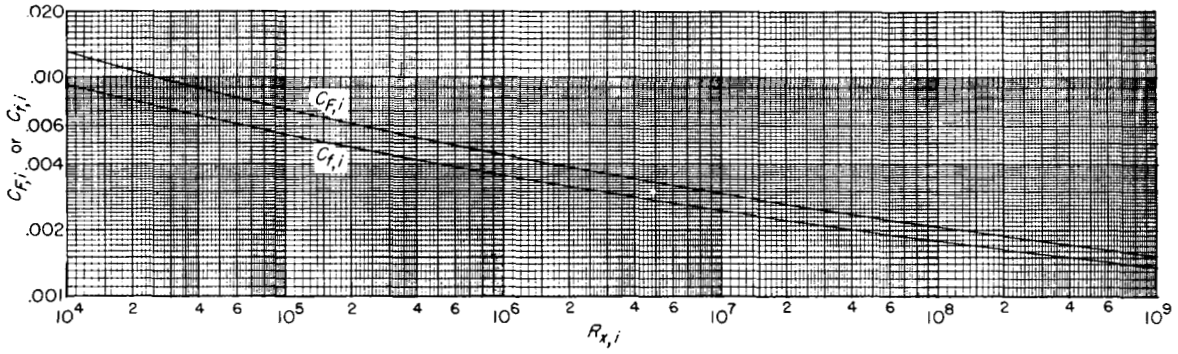

FIGURE 2.—The Karman-Schoenherr values for incompressible turbulent skin friction.

$$R_{\theta,i}=\frac{0.044\ R_{x,i}}{(\log R_{x,i}-1.5)^2} \tag{14}$$

A comparison between the two sets of equations (eqs. (10) and (11) and eqs. (12) and (13)) in the range $10^4<R_{x,i}<10^6$ is shown in figure 3, together with the laminar Blasius equation (9). This graph extends the Sivells and Payne formula below the value of Reynolds numbers for which it was intended. Note that the local skin friction still agrees well with the Karman-Schoenherr equation but the average skin friction starts to deviate from the Karman-Schoenherr equation by a significant amount at the lowest Reynolds numbers.

VALIDATION OF REFERENCE-TEMPERATURE APPROACH

LAMINAR BOUNDARY LAYER

A comparison has been made between average skin friction from the T' method and the Crocco-Van Driest computations presented in reference

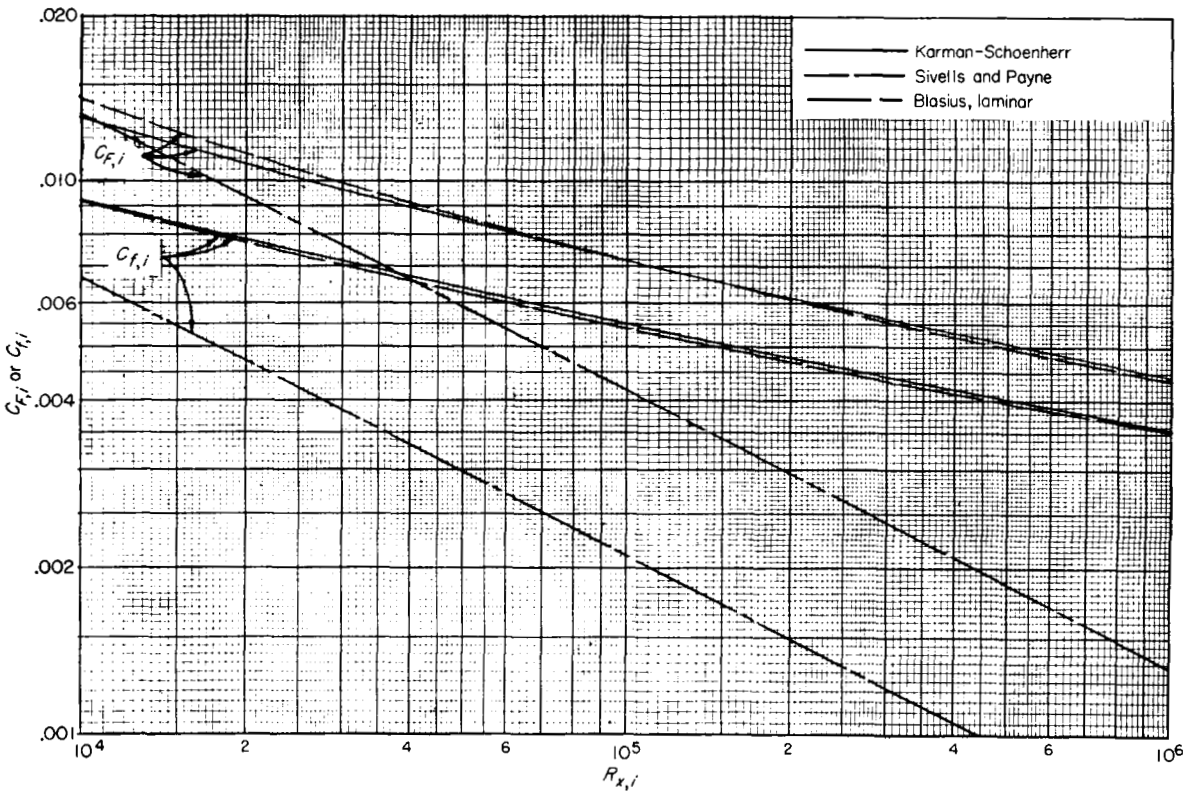

FIGURE 3.—Comparison of the Karman-Schoenherr and Sivells and Payne skin-friction formulas for incompressible turbulent flow and the Blasius equation for incompressible laminar flow.

10. This comparison of average skin-friction parameters with wall temperature is shown in figure 4 for three Mach numbers ($M_\infty=0$, 10, and 20). The T' method, in general, agrees well with the more or less exact Crocco-Van Driest values. The effect of decreasing wall temperature increasing the skin friction is shown at all Mach numbers.

TURBULENT BOUNDARY LAYER

In the case of the turbulent boundary layer some of the available skin-friction data in subsonic and supersonic flow have been used for comparison with computed skin-friction coefficients. However, the experimental points were transformed by the T' equations so that a single comparison could be made with the incompressible results. The viscosity law that was used in transforming the results for air was the Sutherland law and for helium, the power law with an exponent of 0.65.

A comparison of average skin-friction data by Chapman and Kester (ref. 11) with the incompressible formulas is shown in figure 5. These data which were obtained over a Mach number range from 0.5 to 3.6 and transformed to the incompressible form by the T' method agree well with the incompressible curves. As can be seen, however, these data were measured at T' Reynolds numbers from about 10^6 to 3×10^7.

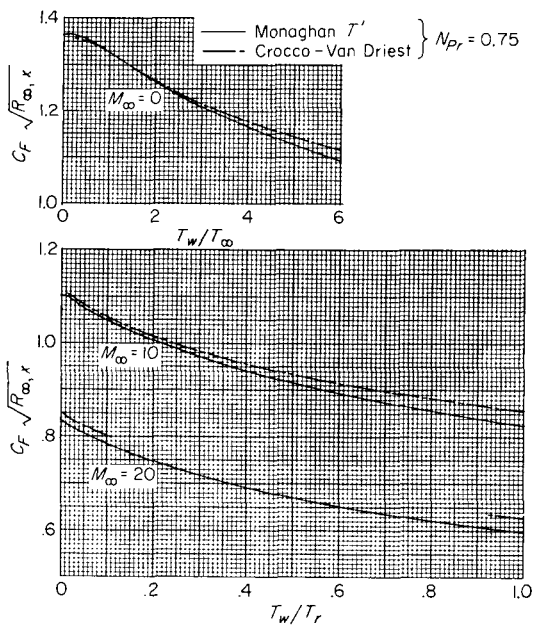

FIGURE 4.—Comparison between computations by the reference-temperature and the Crocco-Van Driest methods for laminar flow.

653982—62——2

Figure 6 carries this comparison to the local skin-friction coefficient as a function of Reynolds number based on distance along the plate utilizing data from references 12 to 14. A greater body of reliable data are available in both air and helium media and the lowest Reynolds number is about 4×10^4. The agreement of the transformed data with the incompressible theories is good except perhaps for a few points at the lowest Reynolds numbers from reference 12 whose accuracy is suspect because the assumed origin of the turbulent boundary layer is approached too closely. Some additional data at a Mach number of about 9 in air were obtained by Hill (ref. 15). The Reynolds numbers for the investigation of reference 15 were evaluated with the momentum thickness as the characteristic length. The transformed local-skin-friction data shown in figure 7 average about 6 percent above the incompressible theories. The lowest equivalent Reynolds number based on x for these data is about 6×10^4 (as can be seen by comparing equivalent $C_{f,i}$ in figs. 6 and 7).

Overall, then, it may be said that the skin-friction data transformed to the incompressible plane according to the T' formulas show good general agreement with the incompressible skin-friction equations (at least for values of R' between about 10^5 and 10^7). Thus, the reverse is implied; the T' method applied to the incompressible formulas can be used to predict compressible results at least over the limited Mach number range where experimental checks have been made. Verification of the very high Mach number calculations that follow awaits experimental evidence.

Values of R', the Reynolds number evaluated at T' conditions, can be lower than the order of 10^4, that is, lower than the lowest Reynolds numbers available for experimental comparison. Shown in figure 8 are the T' Reynolds numbers expressed as ratios to the actual Reynolds numbers over a large range of Mach numbers in both helium and air. Two wall temperatures are shown which are for practical purposes the extremes which are generally dealt with—a wall temperature of absolute zero and the insulated plate (adiabatic wall temperature). Especially with the adiabatic wall temperatures, if the free-stream Reynolds numbers are comparatively low and the Mach numbers high, the T' Reynolds

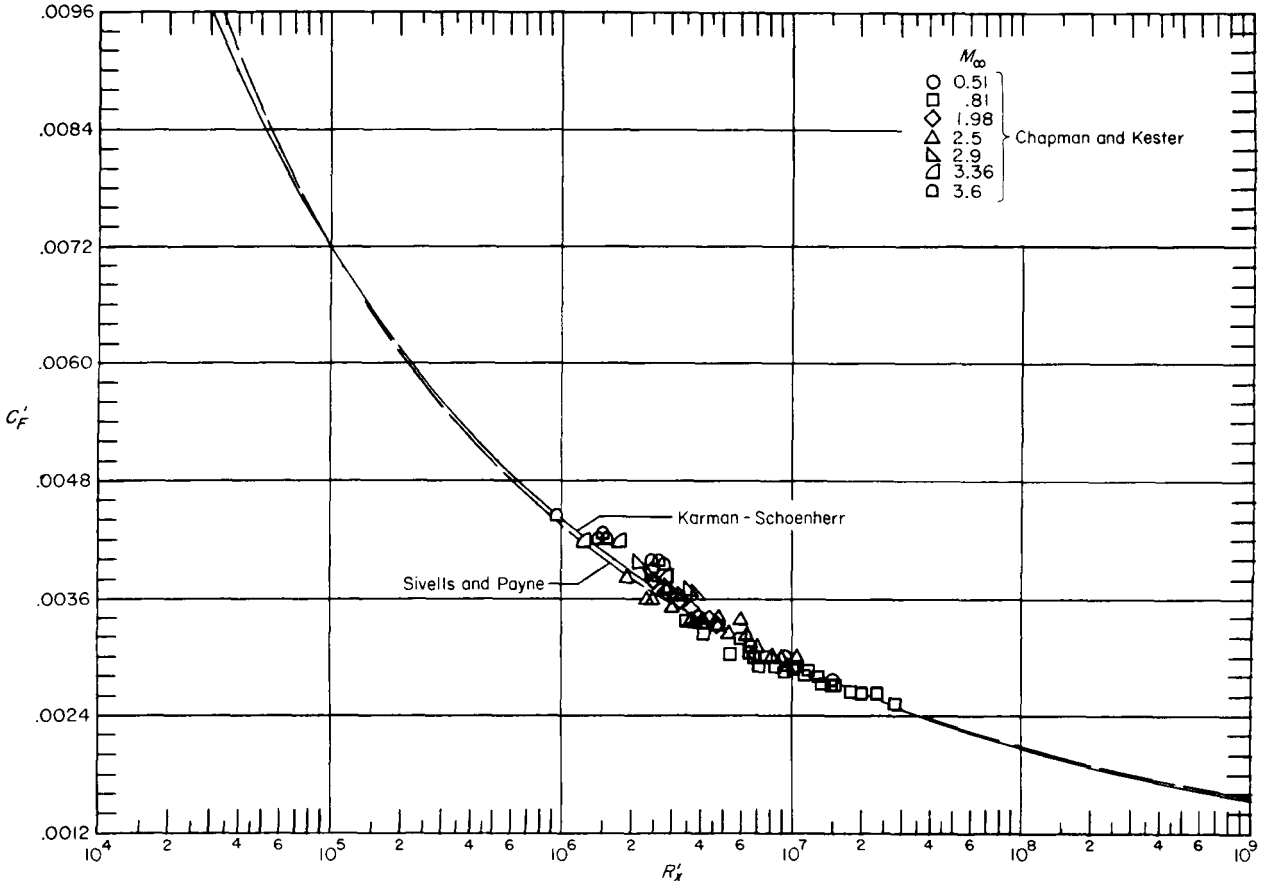

FIGURE 5.—Comparison of experimental results for compressible average turbulent skin friction in reference-temperature form with incompressible formulas.

numbers can be well below the Reynolds numbers at which incompressible data have been obtained. Actually, as can be seen in figure 3 where the T' Reynolds number is below roughly 10^4, the laminar skin friction becomes greater than the turbulent skin friction and it is assumed that the laminar values should be used.

COMPUTATIONS BY REFERENCE-TEMPERATURE METHOD

Based on the Monaghan reference-temperature equations, calculations have been carried out for both laminar and turbulent average skin friction over a flat plate for both $\gamma=7/5$ and $\gamma=5/3$ over the Mach number range from 0 to 30 and the free-stream Reynolds number range from 10^5 to 10^9. For the calculation at $\gamma=7/5$, the Sutherland formula was assumed to hold where

$$\frac{\mu'}{\mu_\infty}=\left(\frac{T'}{T_\infty}\right)^{3/2}\frac{1+\frac{B}{T_\infty}}{\frac{T'}{T_\infty}+\frac{B}{T_\infty}} \tag{15}$$

Values of B/T_∞ were taken as 1.77, 0.50, and 0.125 to represent T_∞ equal 100° R, 396° R, and 1,584° R, respectively. The first static temperature is representative of the free-stream temperature encountered in hypersonic wind tunnels and the last two, of flight temperatures. The temperature of 1,584° R would be encountered at some angle of attack at hypersonic speeds. For the calculations at $\gamma=5/3$, the power formula for viscosity was used by which

$$\frac{\mu'}{\mu_\infty}=\left(\frac{T'}{T_\infty}\right)^{0.65} \tag{16}$$

AVERAGE SKIN FRICTION AS A FUNCTION OF MACH NUMBER

Calculations have been made for the average skin-friction coefficient as a function of Mach number for both the insulated plate and the plate with zero wall temperature. The results of these calculations are shown in figures 9 and 10. Figure 9 is for the insulated flat plate with values of Reynolds number from 10^5 and 10^9 for both laminar and turbulent flow. The average skin-

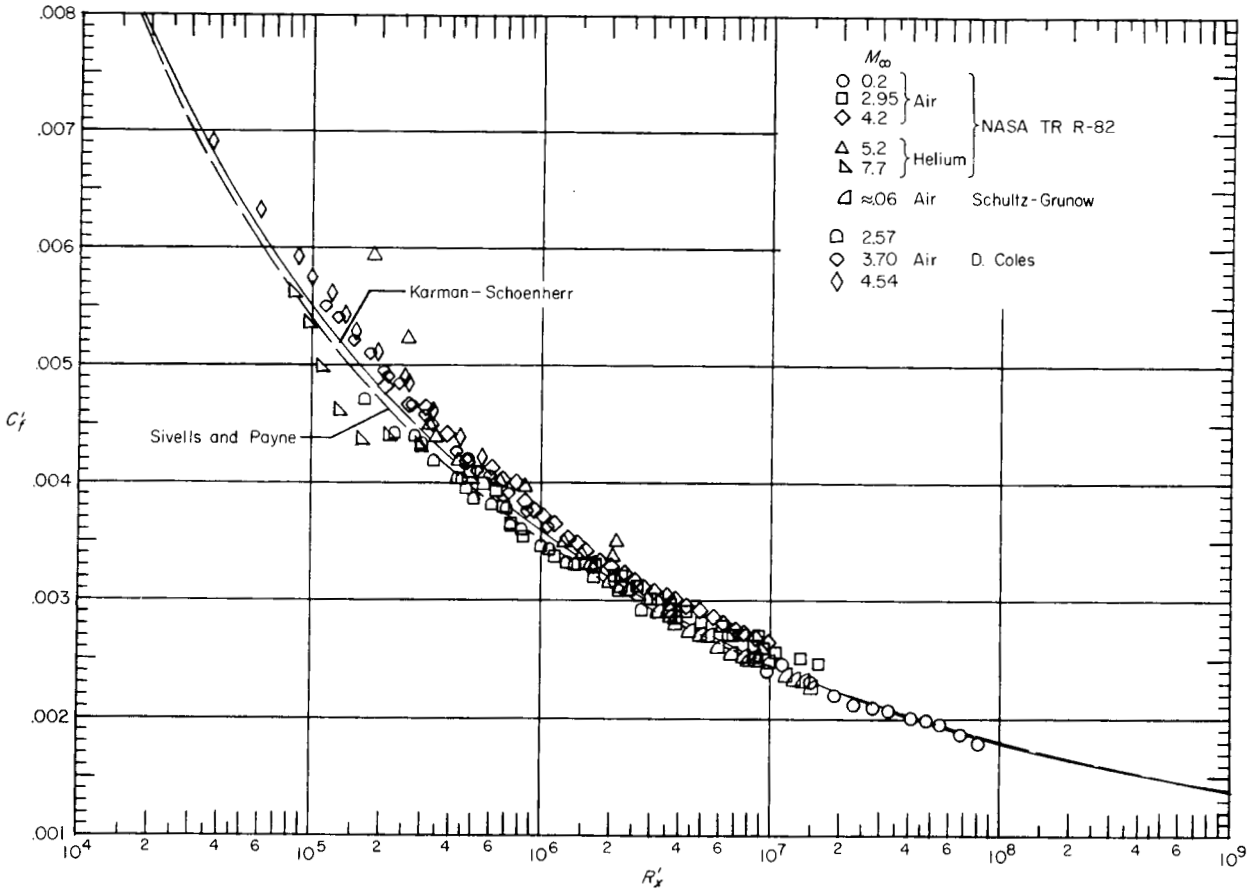

FIGURE 6.—Comparison of experimental results for compressible local turbulent skin friction in reference-temperature form with incompressible formulas.

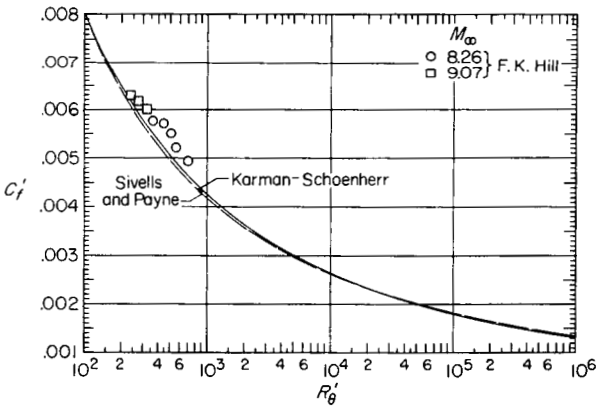

FIGURE 7.—Comparison of experimental results for compressible local turbulent skin friction in reference-temperature form with incompressible formulas utilizing Reynolds number based on momentum thickness.

friction coefficient is presented in the form $C_F/C_{F,i}$ where $C_{F,i}$ is the average incompressible turbulent skin-friction coefficient at the Reynolds number of a particular curve. The incompressible turbulent relation (eq. (12)) was used for all the turbulent computations in this figure. Figures 9(a) to 9(c) are for $\gamma=7/5$ at the three static temperatures and figure 9(d) is for helium. The same conditions apply to figure 10 except that the calculations are for a wall temperature of zero absolute. The familiar effect of a large dropoff in turbulent skin-friction coefficient with increasing Mach number is evident in all these plots together with the relative insensitivity of laminar skin-friction coefficient to Mach number. In addition, when figures 9 and 10 are compared, the turbulent skin-friction coefficient is found to show a much greater increase in skin friction with decreased wall temperature than does the laminar skin friction. The effect of Reynolds number is generally small unless large ranges of Reynolds number are considered.

In order to facilitate an evaluation of the effect of static-temperature level and a comparison between air and helium, the curves for a Reynolds

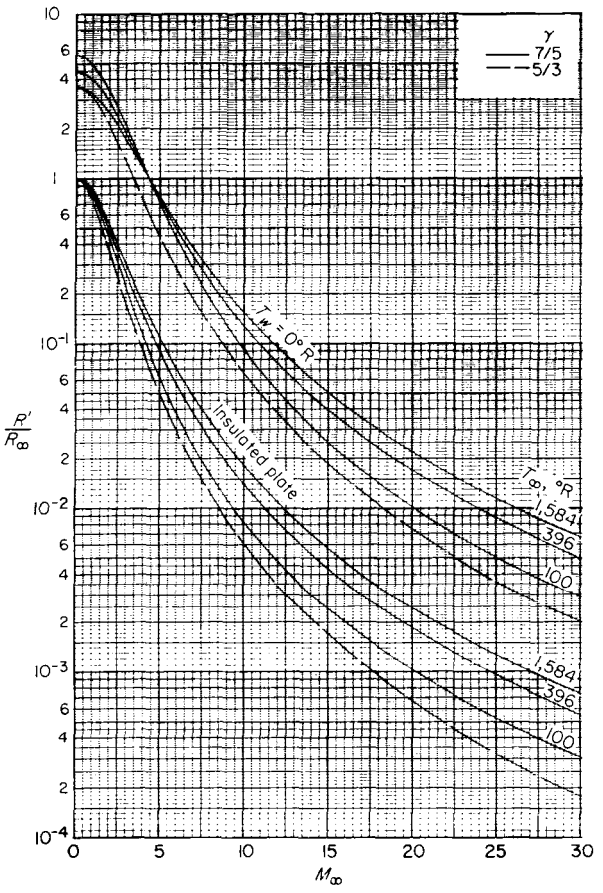

FIGURE 8.—Ratio of reference-temperature Reynolds number for turbulent flow to compressible free-stream Reynolds number as a function of Mach number for air and helium.

number of 10^8 from figures 9 and 10 have been included in figure 11. This graph shows a larger effect of free-stream temperature level on skin friction in laminar flow than in turbulent flow, the relative effect not being affected much by wall temperature. (Compare figs. 11(a) and 11(b).)

For laminar flow figure 11 shows that C_F is roughly equal in air and helium for a static temperature of about 400° R at the same Mach number. For turbulent flow, however, the value of C_F in helium is considerably below that in air but is roughly equal to that in air for the same value of k or $M_{helium}/M_{air} \approx 0.775$. This result was shown previously in reference 16; however, in those results no effect of Reynolds number on the ratio $C_F/C_{F,i}$ was found since the power law for skin friction was utilized. (See figs. 9 and 10.)

AVERAGE SKIN FRICTION AS AFFECTED BY WALL TEMPERATURE

The preceding presentation has shown the effect of Mach number on the average skin friction for the insulated plate and for the case of zero wall temperature. There is a significant difference between these two cases for turbulent flow; thus, it appears important to determine skin friction as a function of wall temperature. Calculations were made for a few values of Mach number for both air and helium. The results for turbulent flow are shown in figure 12 for $R_{\infty,x}=10^8$ and $T_\infty=100°$ R in air. (Refer to fig. 4 for the effect of wall temperature in laminar flow.) The skin friction at the wall temperature T_w is shown in ratio to the skin friction for an insulated plate and plotted against the ratio of wall temperature to insulated-plate temperature. There is, in general, a much greater effect of a change in wall temperature at very low wall temperatures than when the wall temperature is close to the adiabatic value. The results of the air and helium calculations are much the same.

Calculations were also made to evaluate the effects of free-stream temperature level and Reynolds number at various wall-temperature levels. These calculations for $\gamma=7/5$ are plotted in figure 13. The free-stream temperature level has only a small effect on the skin-friction ratio plotted. The effect of Reynolds number is not judged to be important.

EFFECT OF CHOICE OF TURBULENT INCOMPRESSIBLE SKIN-FRICTION LAW ON COMPUTATIONS

The curves in figures 9 to 11 were computed by using the incompressible turbulent relation of Sivells and Payne (eq. (12)). In order to determine how much effect this choice of law might have as compared with the Karman-Schoenherr law (eq. (10)) sample computations were made by using equation (10) and were compared with those made by using equation (12). The result is shown in figure 14. The results obtained by the two methods are practically identical except at the highest Mach number for each value of $R_{\infty,x}$ corresponding to values of R'_x of roughly 10^4 (see fig. 8) where C'_F by the two formulas depart from each other (see fig. 3). Even at its worst, however, the deviation between the two computations shown in figure 14 is not large.

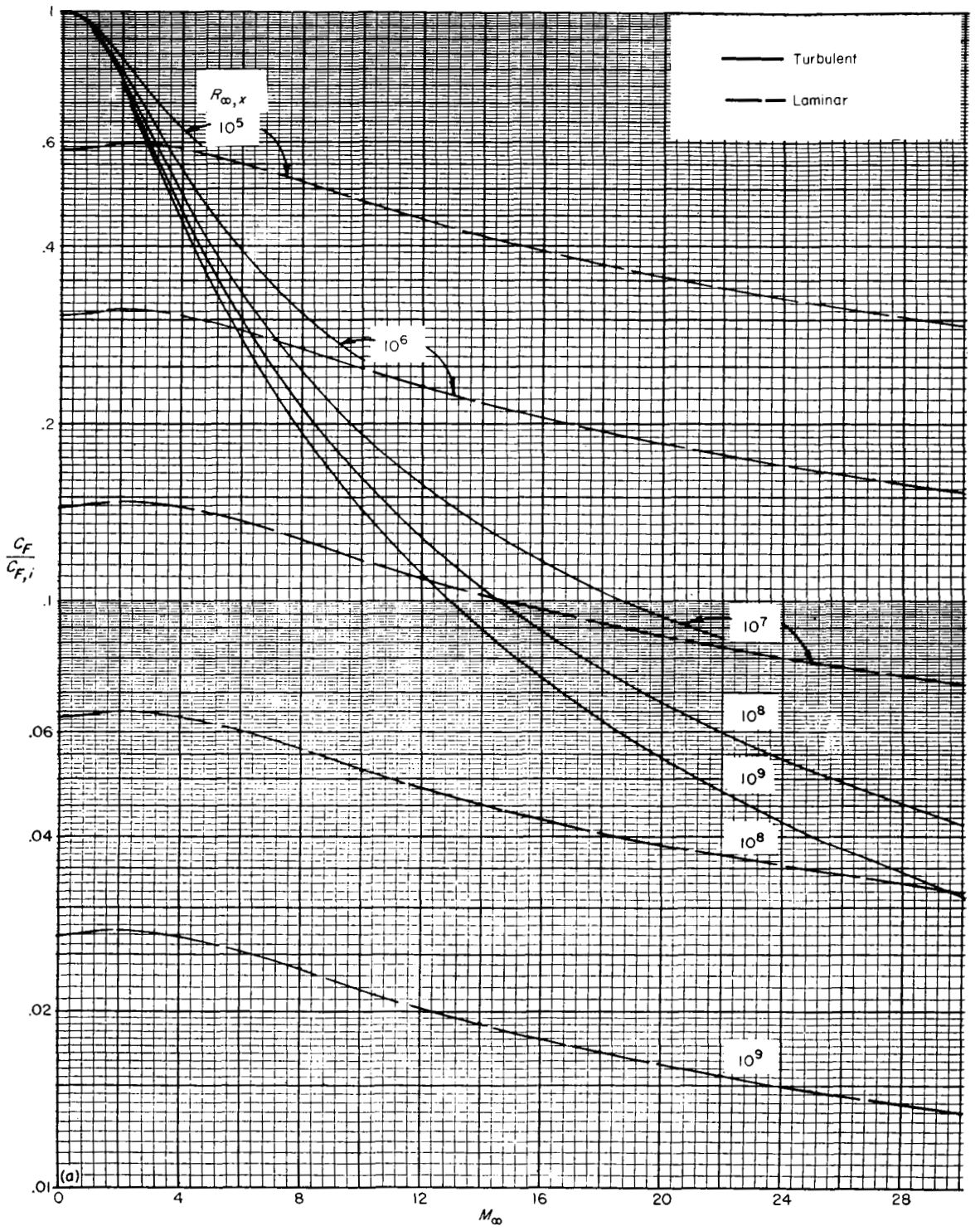

(a) $\gamma=7/5$ (air); $T_\infty=100°$ R.

FIGURE 9.—Ratio of compressible average skin friction to turbulent incompressible average skin friction as a function of Mach number. Insulated plate.

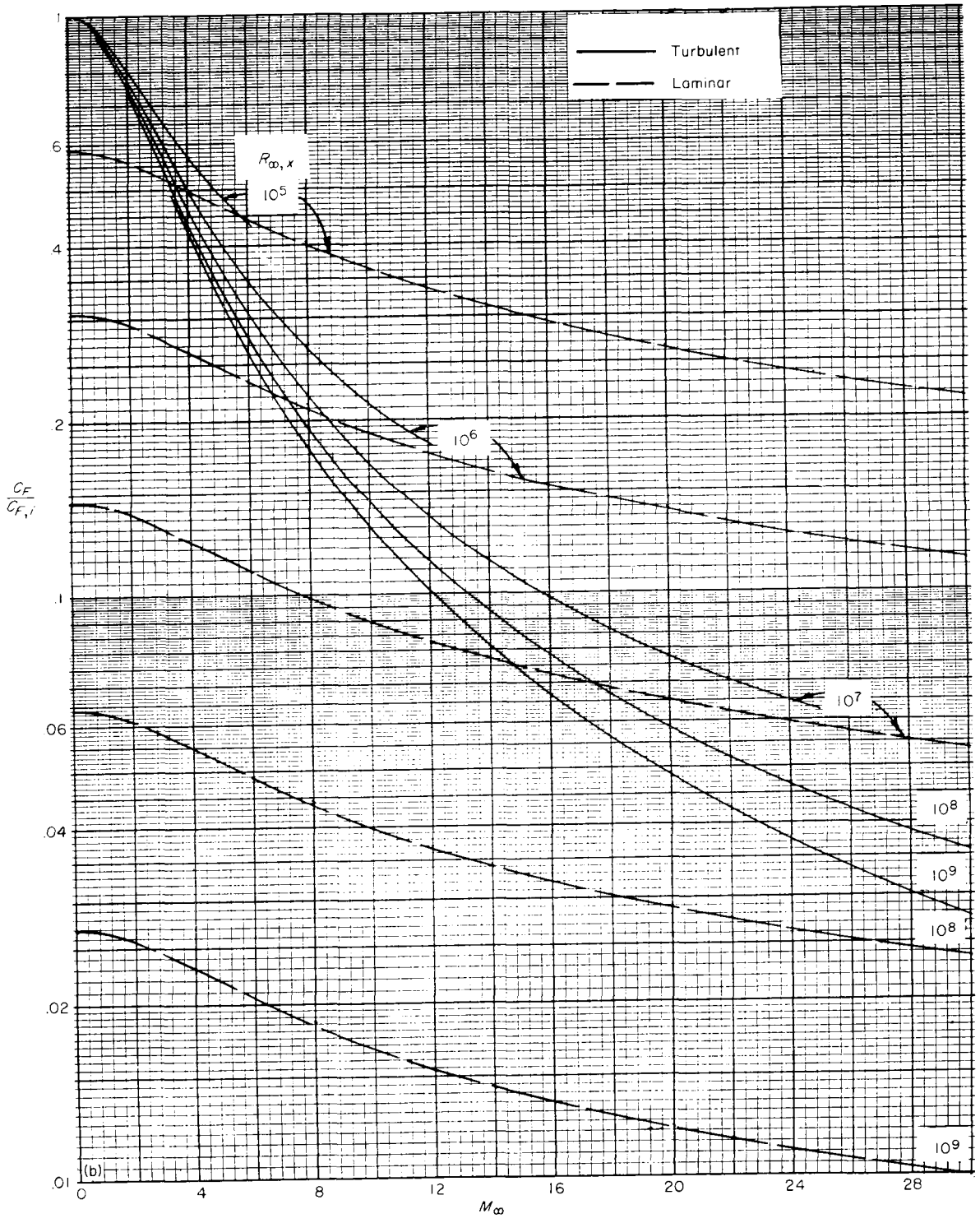

(b) $\gamma=7/5$ (air); $T_\infty=396°$ R.

FIGURE 9.—Continued.

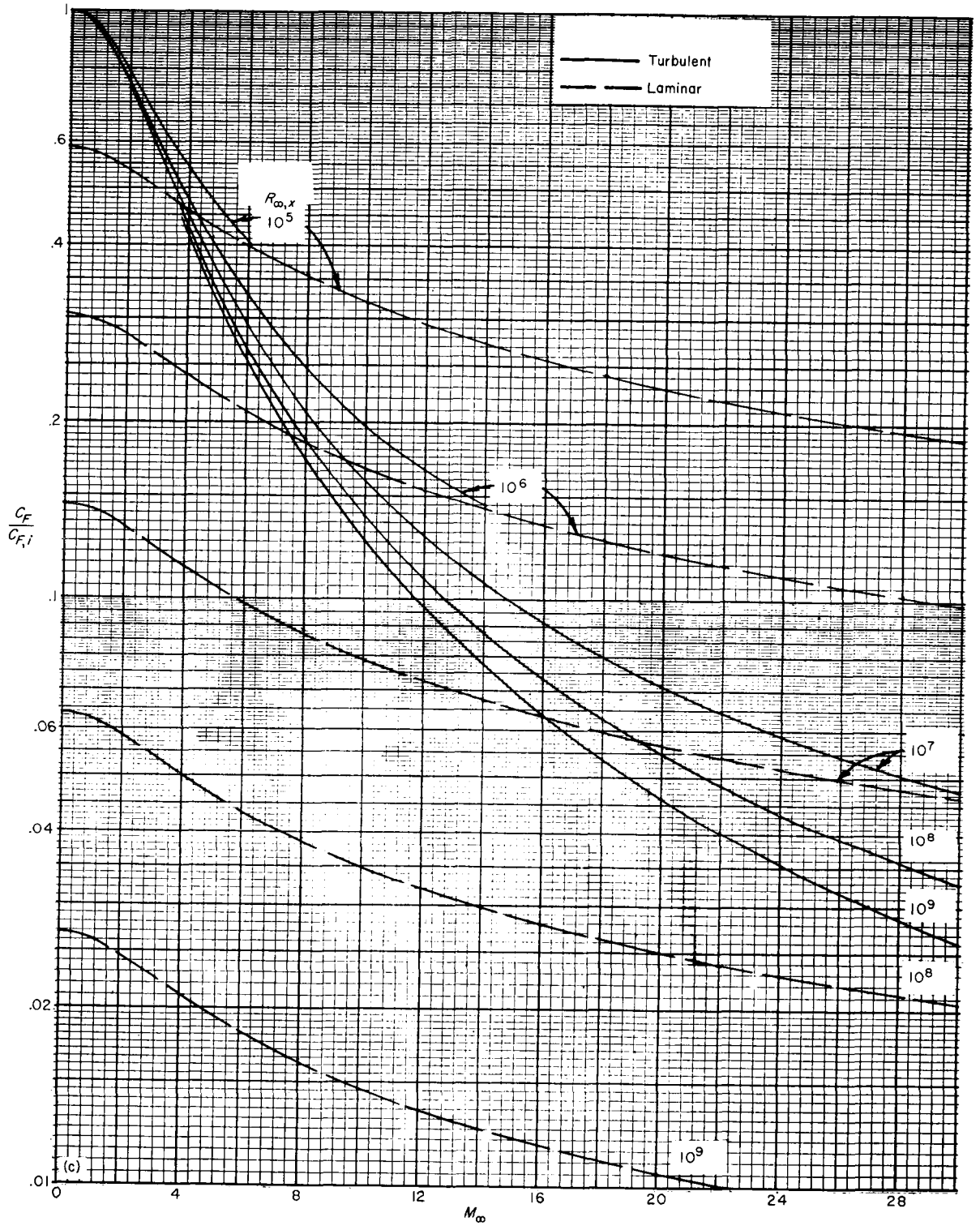

(c) $\gamma = 7/5$ (air); $T_\infty = 1{,}584°$ R.

FIGURE 9.—Continued.

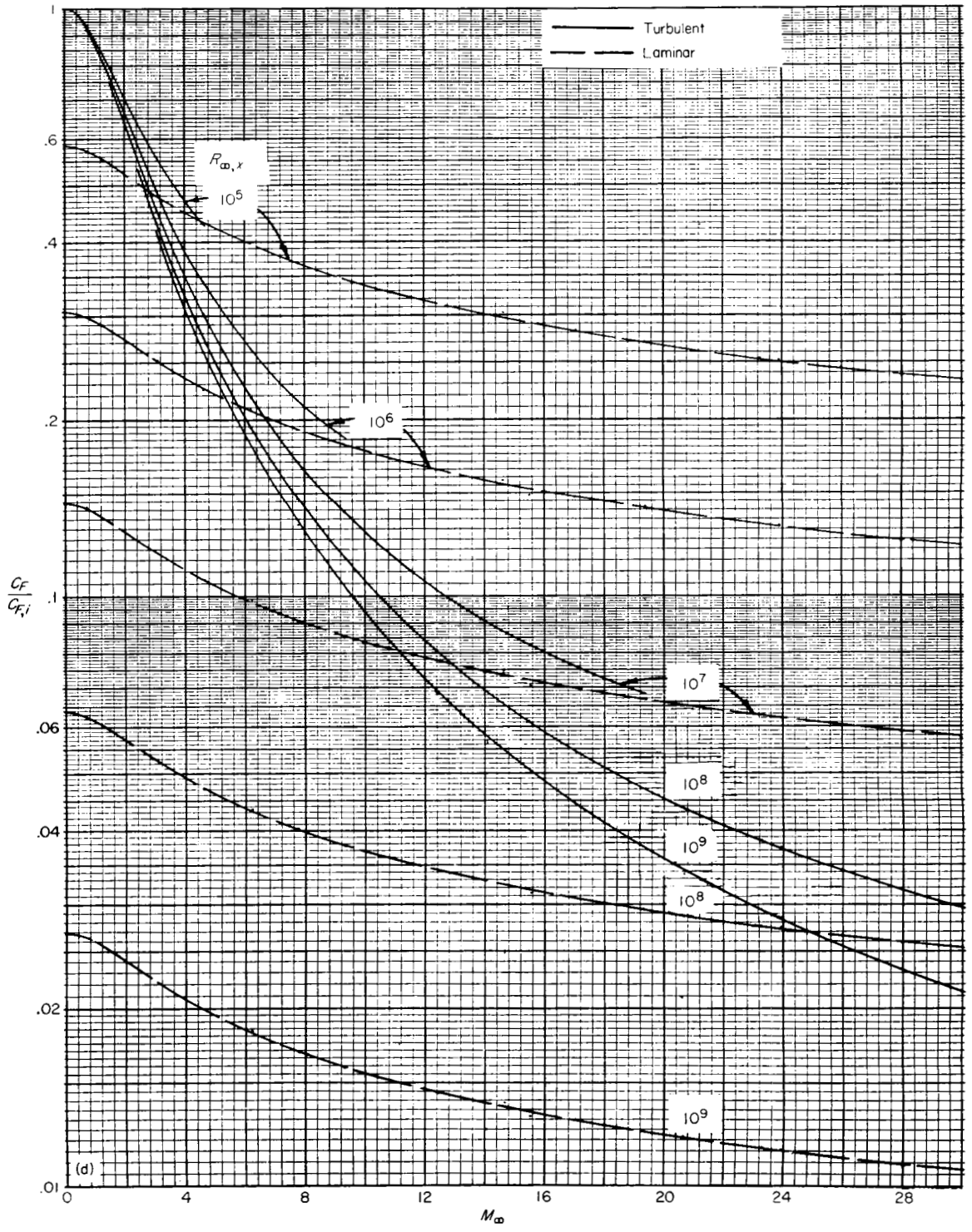

(d) $\gamma=5/3$ (helium); $\omega=0.65$.

FIGURE 9.—Concluded.

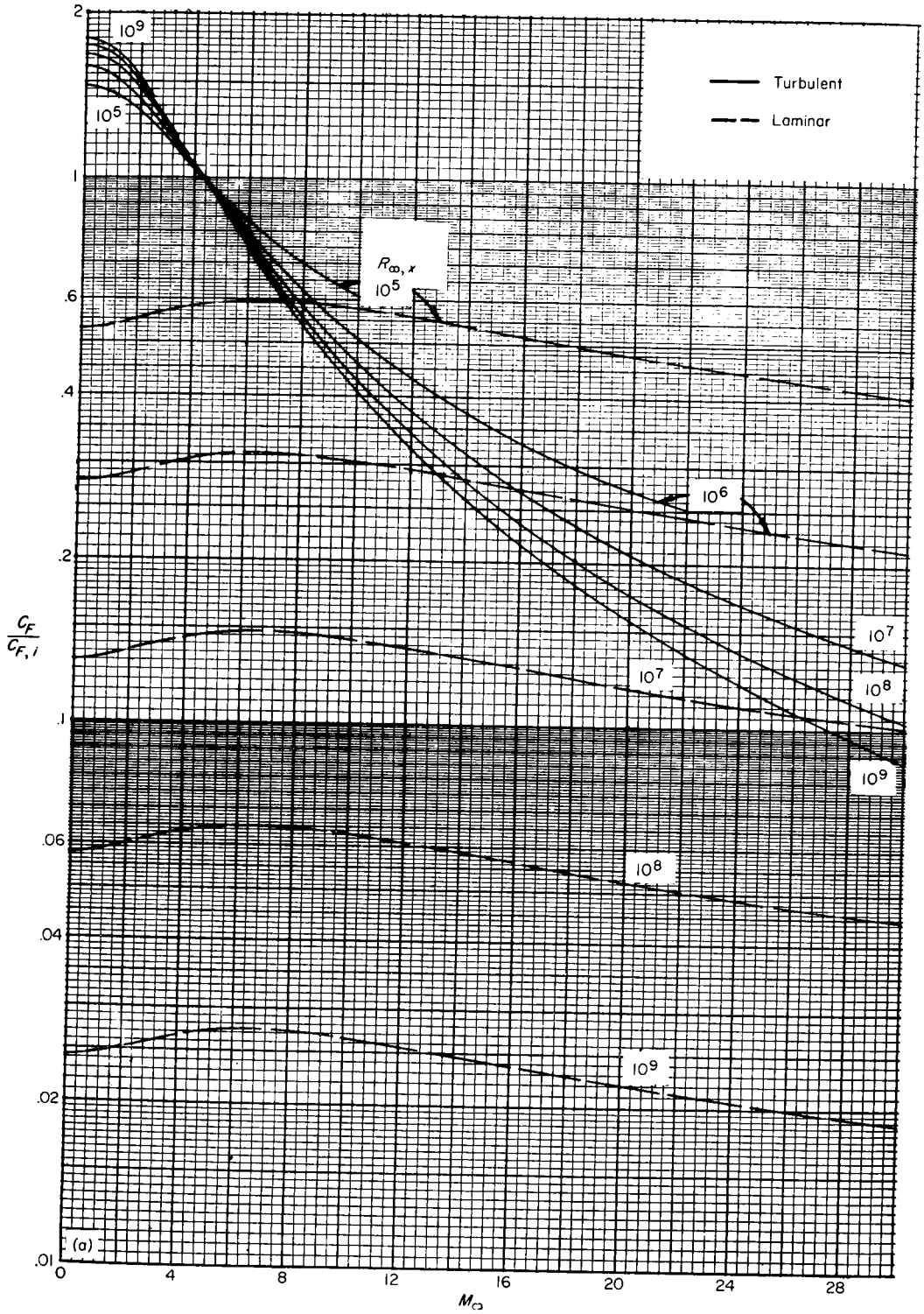

(a) $\gamma = 7/5$ (air); $T_\infty = 100°$ R.

FIGURE 10.—Ratio of compressible average skin friction to turbulent incompressible average skin friction as a function of Mach number. $T_w = 0°$ absolute.

653982—62——3

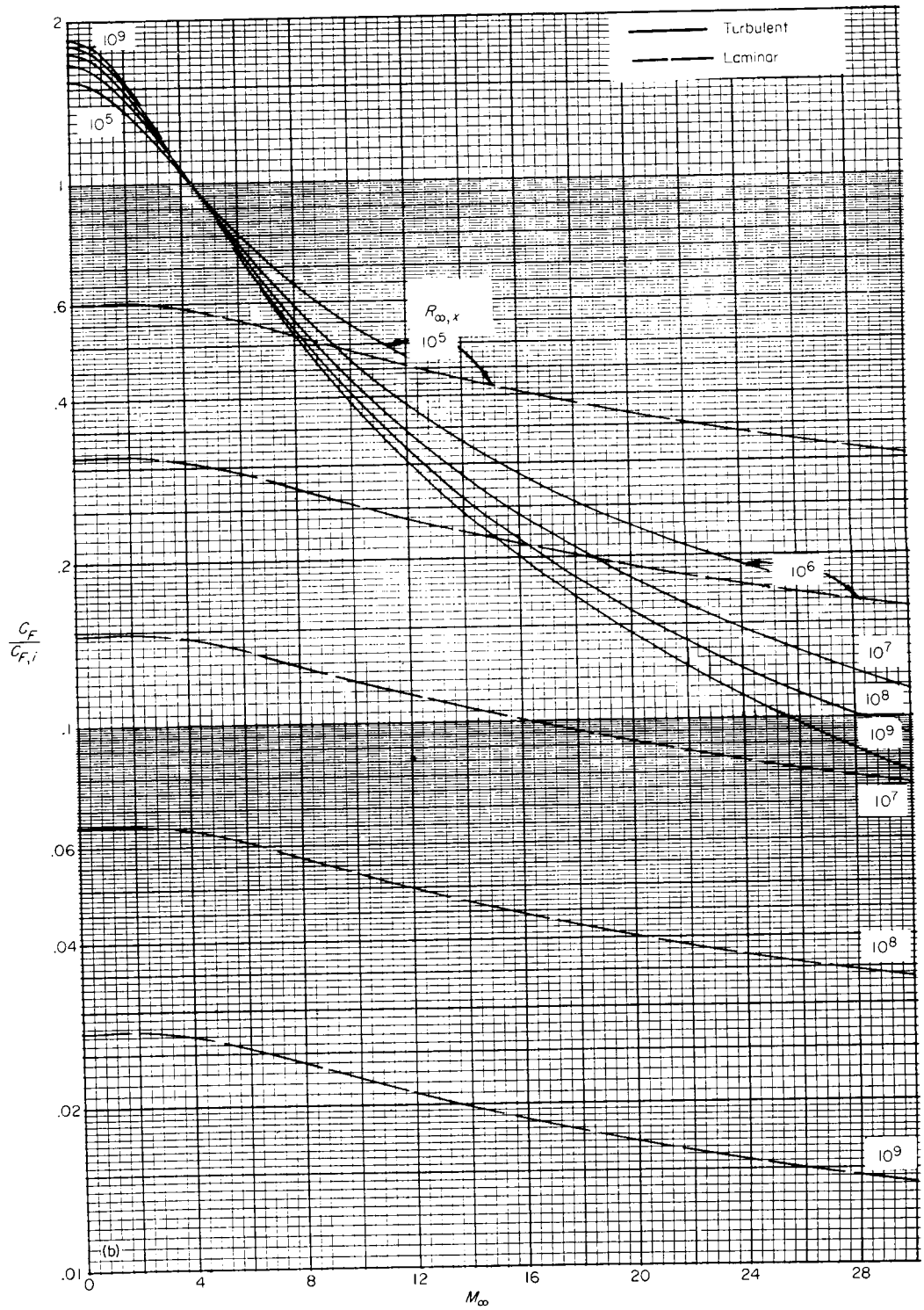

(b) $\gamma=7/5$ (air); $T_\infty=396°$ R.

FIGURE 10.—Continued.

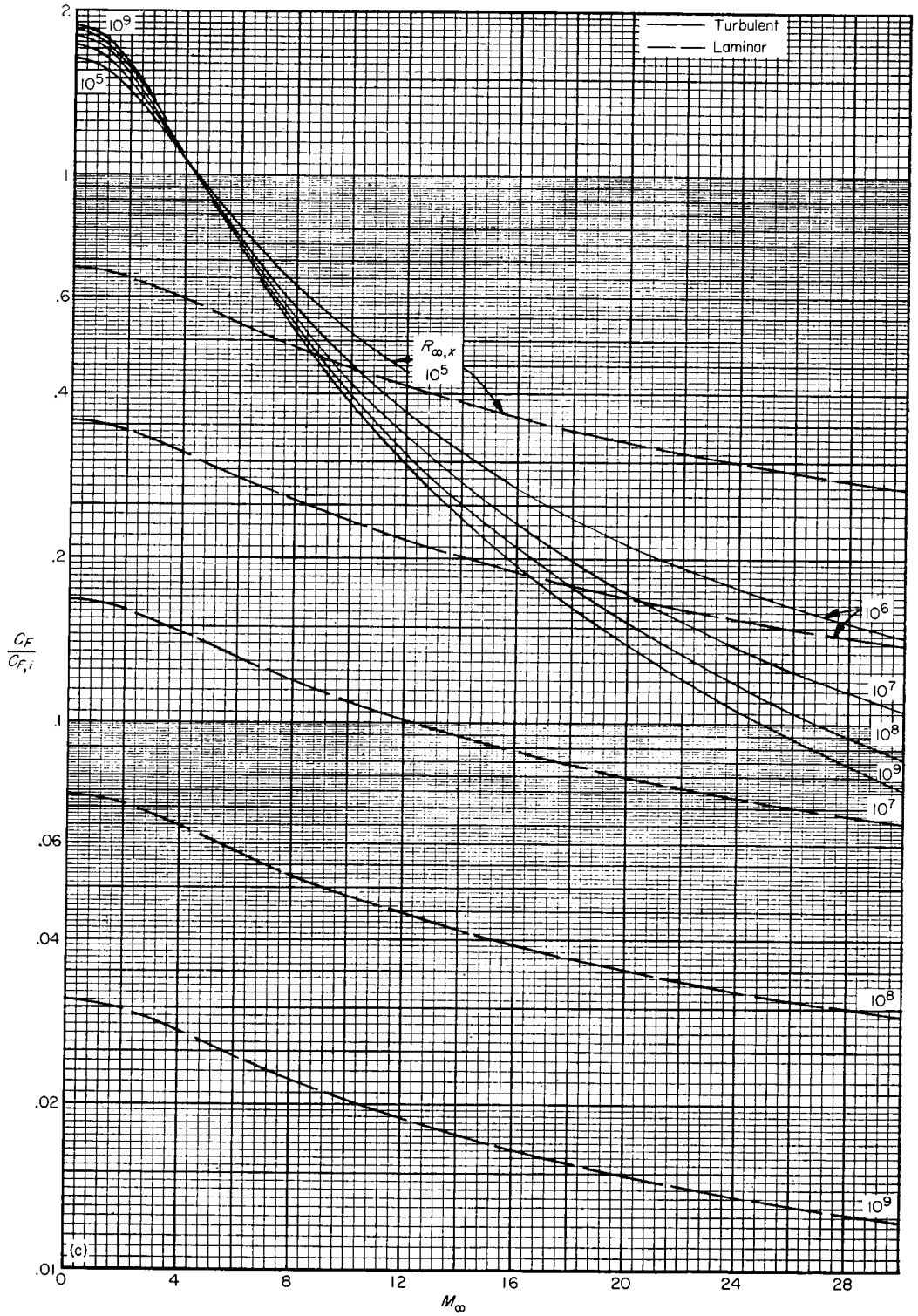

(c) $\gamma=7/5$ (air); $T_\infty=1{,}584°$ R.

FIGURE 10.—Continued.

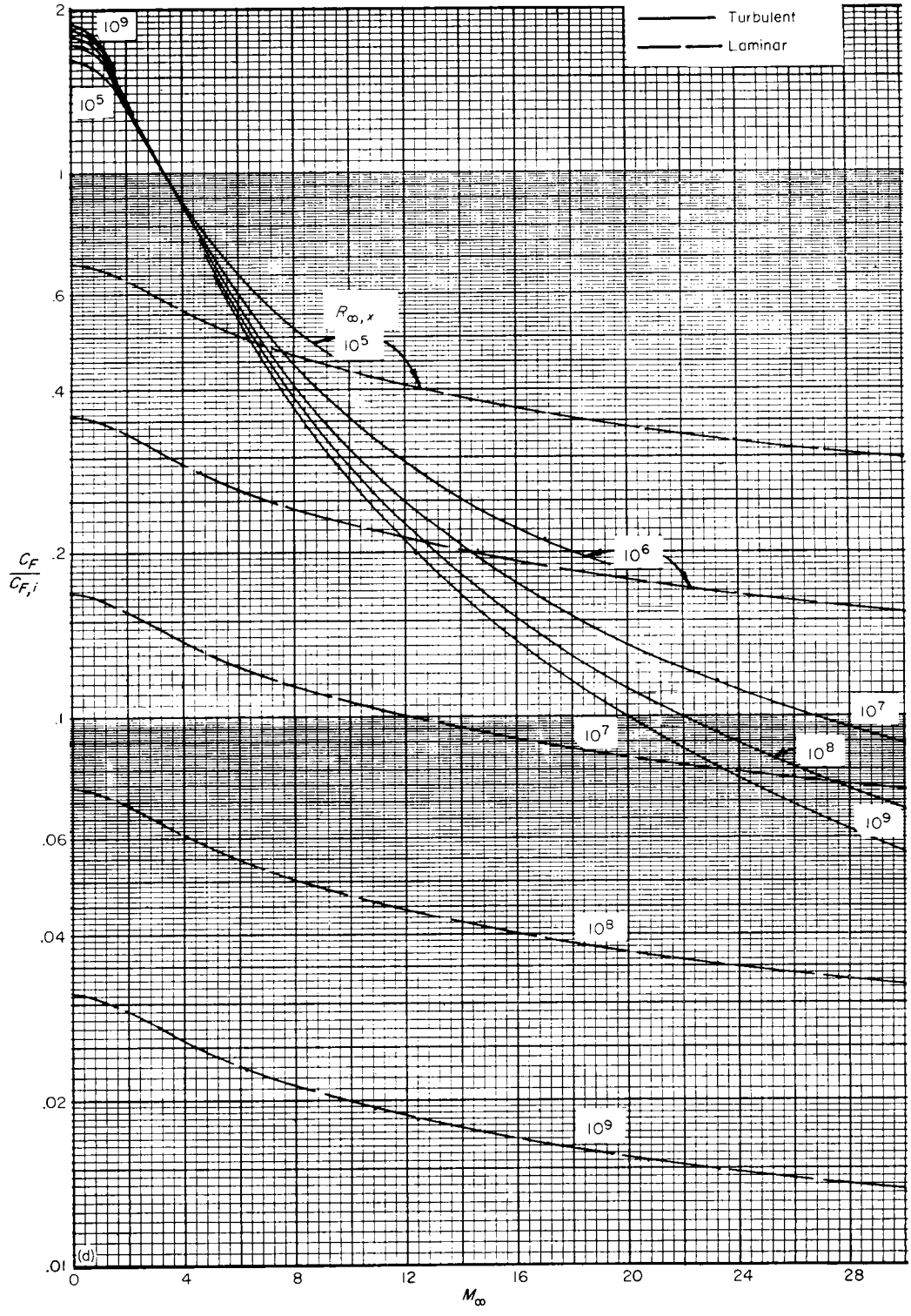

(d) $\gamma=5/3$ (helium); $\omega=0.65$.

FIGURE 10.—Concluded.

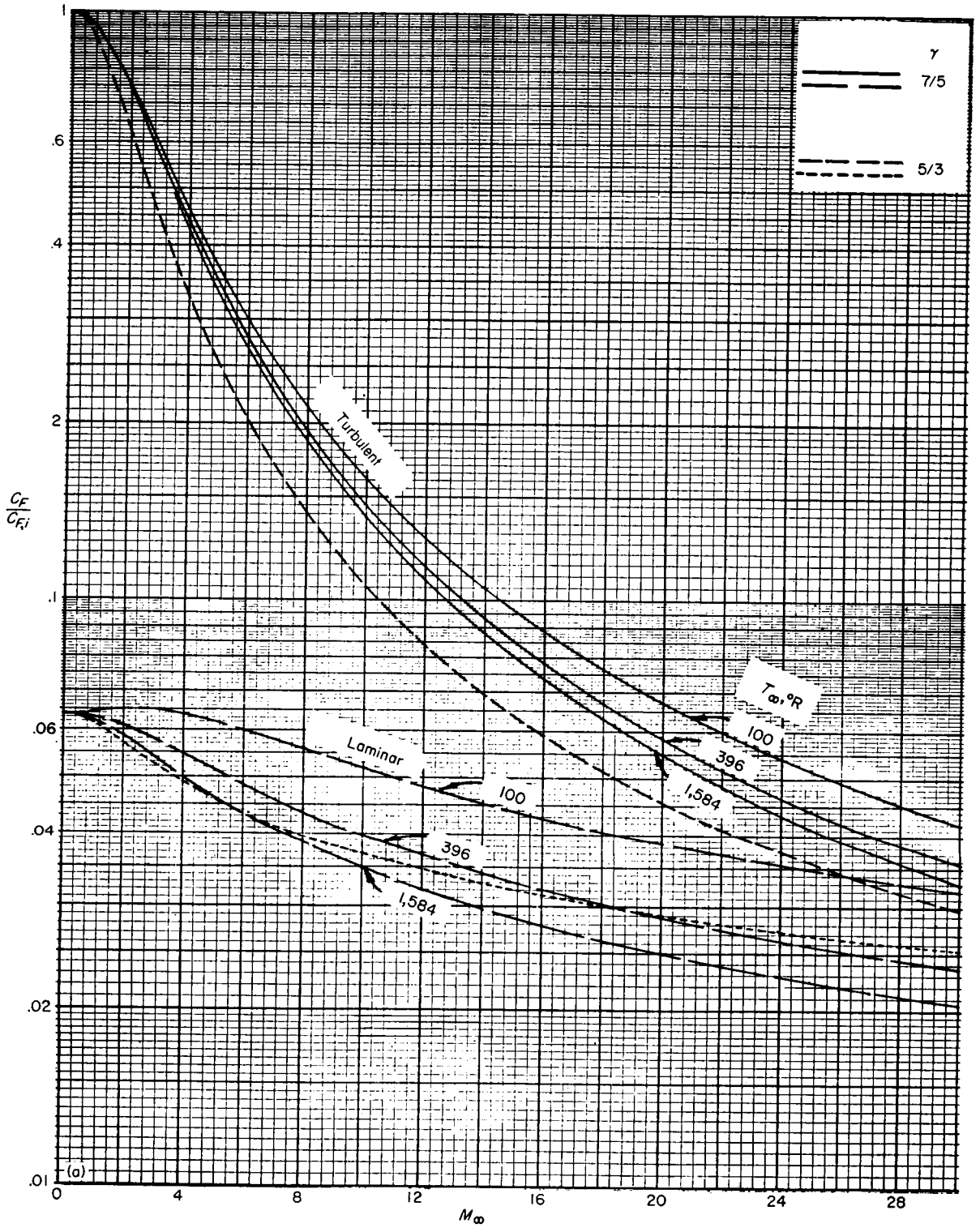

(a) Insulated plate.

FIGURE 11.—Ratio of compressible average skin friction to turbulent incompressible average skin friction for $\gamma=7/5$ (air) at various free-stream temperature levels and for $\gamma=5/3$ (helium). $R_{\infty,x}=10^8$.

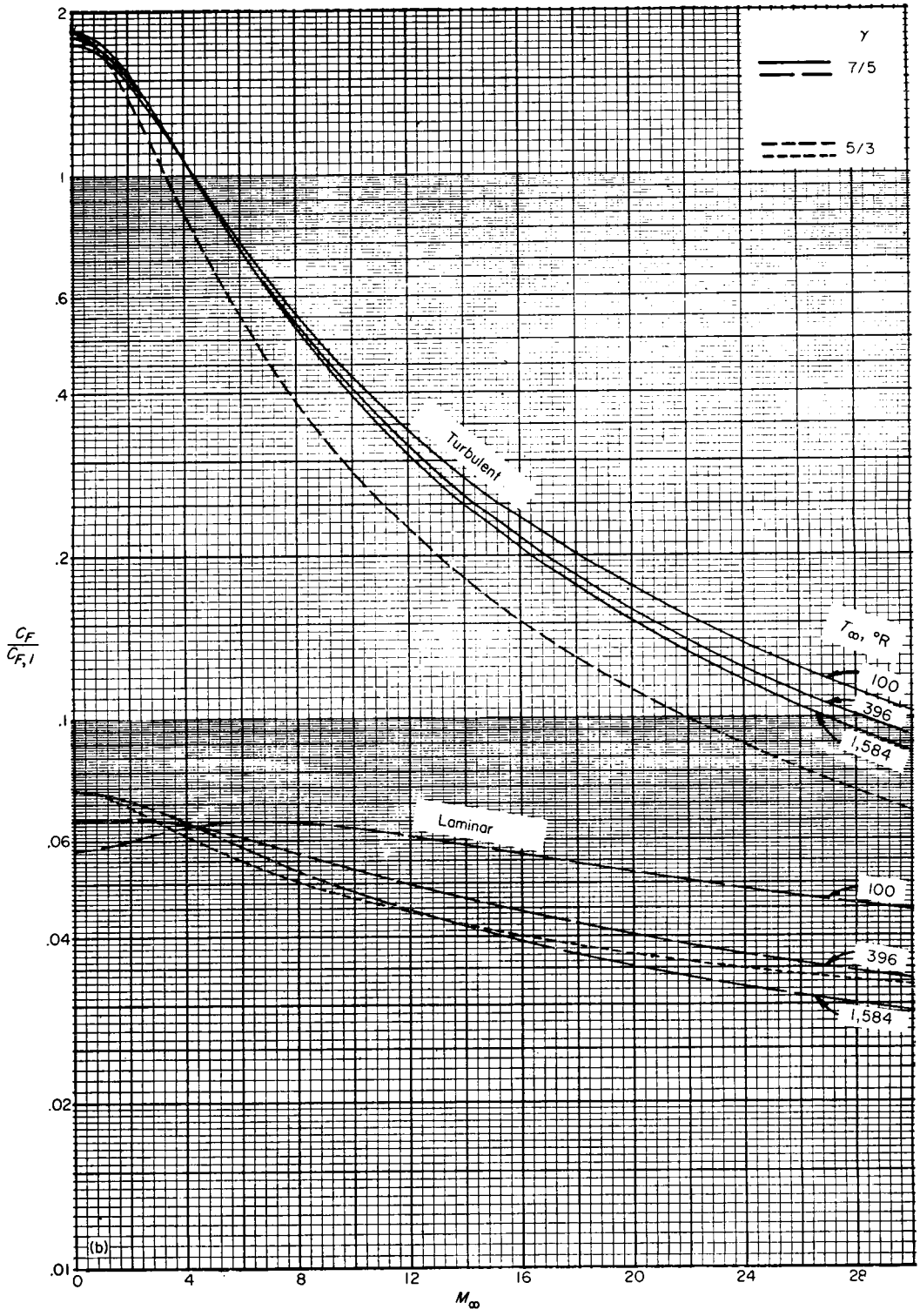

(b) $T_w = 0°$ absolute.

FIGURE 11.—Concluded.

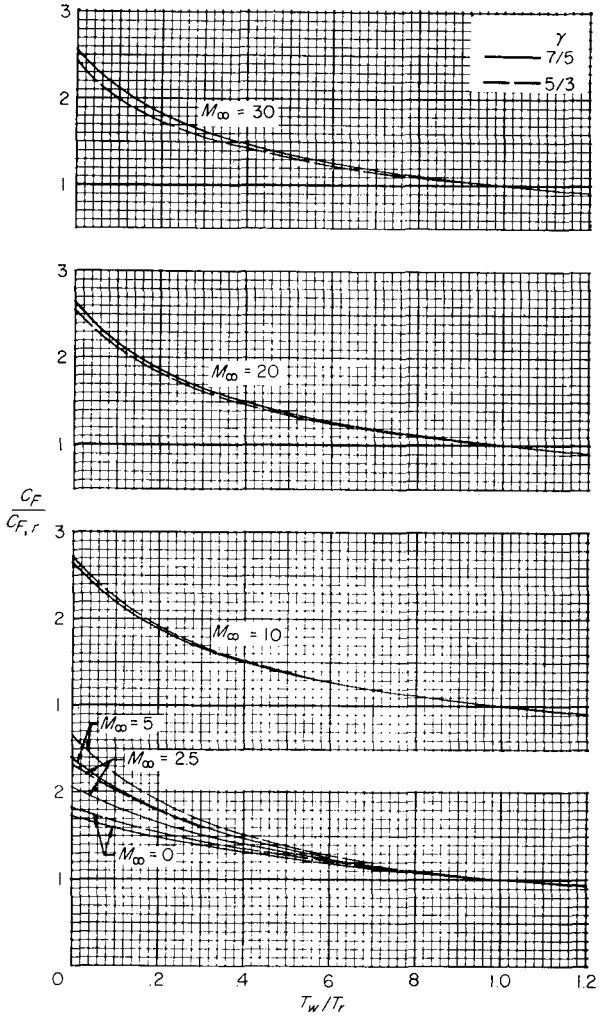

FIGURE 12.—Effect of wall temperature on average turbulent skin friction for various Mach numbers in the range from 0 to 30. $R_{\infty,x}=10^8$; air ($T_\infty=100°$ R) and helium.

It should be mentioned that the objection to use of the Karman-Schoenherr formulas of $C_{F,i}$, being nonexplicit in terms of $R_{x,i}$, was removed for practical purposes when it was found that reference 7 contained a table of the Karman-Schoenherr values of $C_{F,i}$. These tabulated values are given in increments of $R_{x,i}$ of 0.01×10^m where m varies from 5 to 10. This table, however, was not discovered until a large number of the computations had been done. Reference 7 also contains a good comparison of a number of proposed incompressible turbulent skin-friction laws.

Because of its inherent simplicity, the power

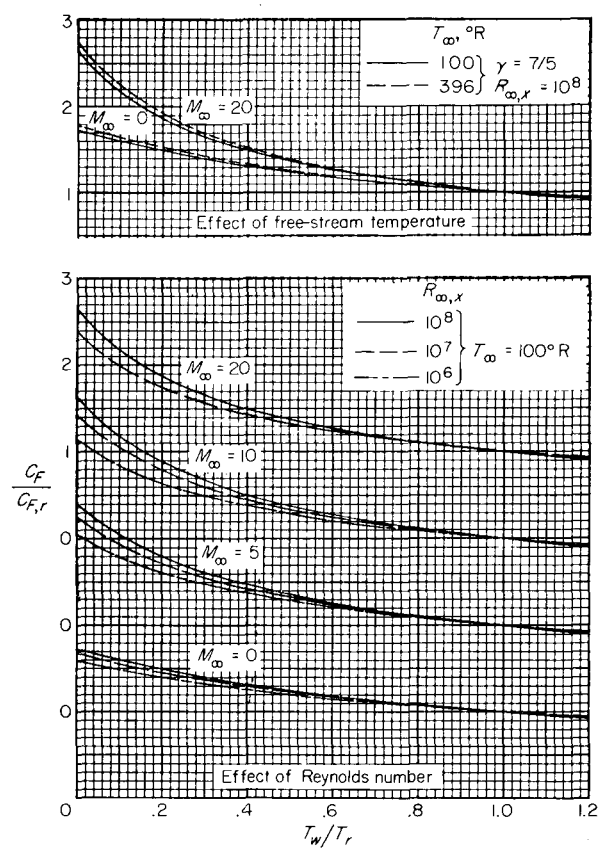

FIGURE 13.—Effect of wall temperature, free-stream temperature, and Reynolds number on average turbulent skin friction at various Mach numbers in air.

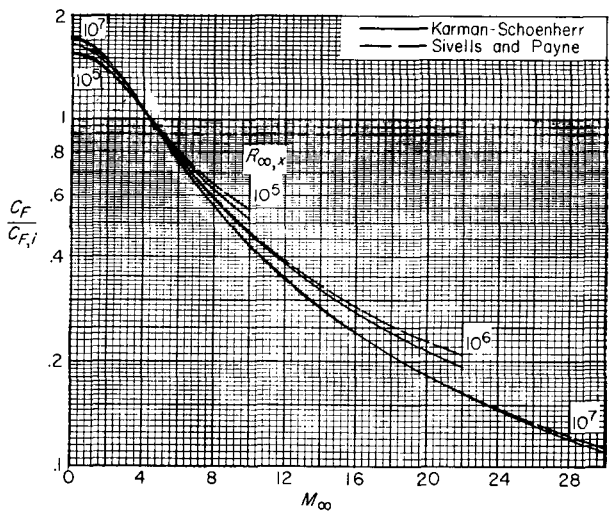

FIGURE 14.—Effect of utilization of two different turbulent incompressible average skin-friction formulas for computing compressible skin friction by the reference-temperature method. $\gamma=7/5$ (air); $T_w=0°$ absolute; $T_\infty=396°$ R.

law for skin friction is often utilized as an aid to rapid calculations and evaluations of theoretical trends. For example, a comparison of the turbulent skin friction of air and helium was made in the previous section and it was pointed out that the present analysis gave much the same result as that obtained in reference 16. However, reference 16 uses the considerably simplifying assumption that the power law holds for turbulent skin friction where

$$C_{F,i}=aR_{x,i}^{n} \tag{17}$$

and the value of n was assumed to be $-1/5$. It is of interest to examine the values of n which are given by equations (10) to (13). In this case the local values of the exponent n will be examined since these values are relatively simple to obtain analytically.

For any function (for example, $f(x)$) the local value of the exponent in a power-law fit to the function may be expressed as $n=xf'(x)/f(x)$. Thus for the Karman-Schoenherr relations (eqs. (10) and (11))

$$n(C_{F,i})=-\frac{0.8686}{\frac{0.242}{\sqrt{C_{F,i}}}+0.8676} \tag{18}$$

$$n(C_{f,i})=n(C_{F,i})\frac{0.242+0.4343\sqrt{C_{F,i}}}{0.242+0.8686\sqrt{C_{F,i}}} \tag{19}$$

and for the Sivells and Payne relations (eqs. (12) and (13))

$$n(C_{F,i})=-\frac{0.8686}{\log R_{x,i}-1.5} \tag{20}$$

$$n(C_{f,i})=-\frac{0.8686\log R_{x,i}+2.435}{(\log R_{x,i}-1.5)(\log R_{x,i}-2.3686)} \tag{21}$$

Examination of figure 2 indicates that the local value of n at a given Reynolds number allows a fairly accurate power-law fit to more precise turbulent laws for about one decade in Reynolds number on either side of the given Reynolds number. A graph of equations (18) to (21) is shown in figure 15 in which the inverse of n is shown in order to deal with integral numbers rather than fractions. Most evident is the result that the local value of $1/n$ can vary markedly from a value of -5; thus, large variations in Reynolds number can cause appreciable errors in analyses which assume a constant value of n.

EFFECT OF NORMAL SHOCK AT LEADING EDGE ON SKIN FRICTION

For actual use at hypersonic speeds most wings would be blunted. If some simplifying assumptions are made, the effect of this blunting can be assessed. In the calculations the boundary layer is assumed to be growing in a uniform flow which has undergone a normal shock after which it has been expanded to conditions designated 3. Under this assumption the Mach number outside the boundary layer may be readily found. With the assumption that the undisturbed free-stream Mach number $M_\infty \gg 1$, the following simplified equation is obtained for the Mach number M_3:

$$M_3=\sqrt{\frac{2}{\gamma-1}\left[\left(\frac{\gamma+1}{2}\right)^{\frac{\gamma+1}{\gamma}}\left(\frac{1}{\gamma}\right)^{1/\gamma}\left(\frac{M_\infty^2}{p_3/p_\infty}\right)^{\frac{\gamma-1}{\gamma}}-1\right]} \tag{22}$$

For $\gamma=7/5$,

$$M_3=2.318\sqrt{\left(\frac{M_\infty^2}{p_3/p_\infty}\right)^{0.2857}-0.9302} \tag{22a}$$

For $\gamma=5/3$,

$$M_3=1.870\sqrt{\left(\frac{M_\infty^2}{p_3/p_\infty}\right)^{0.4000}-0.8576} \tag{22b}$$

and $M_3=1$ where

$$\frac{p_3/p_\infty}{M_\infty^2}=\left(\frac{\gamma+1}{2\gamma}\right)^{\frac{1}{\gamma-1}}$$

The values of M_3 given by equation (22) are shown in figure 16 for $\gamma=7/5$ and $\gamma=5/3$ where M_3 is plotted as a function of the parameter $\frac{p_3/p_\infty}{M_\infty^2}$. Even though equation (22) is based on the assumption that $M_\infty \gg 1$, the error in M_3 is only about 1 percent at a value of M_∞ as low as 3 with $p/p_\infty=1$.

In a similar manner the local Reynolds number may be obtained. Again with $M_\infty \gg 1$ and a normal shock, after which there is an expansion to conditions 3, the following relation is obtained:

$$\frac{\rho_3 u_3}{\rho_\infty u_\infty}\equiv\frac{R_3}{R_\infty}\frac{\mu_3}{\mu_\infty}=\frac{p_3/p_\infty}{M_\infty^2}M_3\sqrt{\frac{2}{\gamma-1}\left(1+\frac{\gamma-1}{2}M_3^2\right)} \tag{23}$$

Results from equation (23) utilizing equation (22) for M_3 are shown in figure 17(a).

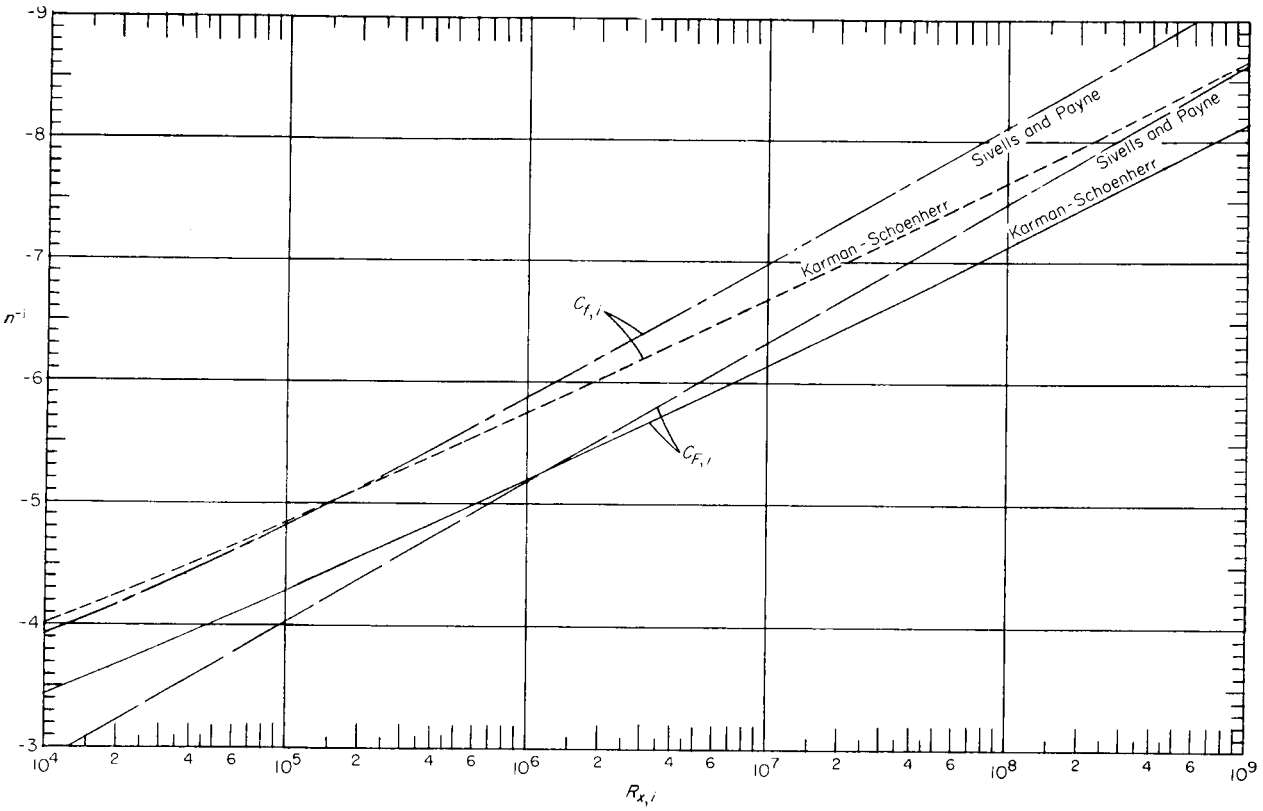

FIGURE 15.—Local value of the inverse of the exponent in a power-law fit to the turbulent incompressible skin-friction formulas.

For air where the Sutherland viscosity equation well represents the available data, then equivalent to equation (15)

$$\frac{\mu_3}{\mu_\infty}=\left(\frac{T_3}{T_\infty}\right)^{3/2}\frac{1+\frac{B}{T_\infty}}{\frac{T_3}{T_\infty}+\frac{B}{T_\infty}} \tag{24}$$

In helium the viscosity is better represented by a power law

$$\frac{\mu_3}{\mu_\infty}=\left(\frac{T_3}{T_\infty}\right)^{\omega} \tag{25}$$

which to the approximation employed may be written as

$$\frac{\mu_3}{\mu_\infty}=\left[\frac{\frac{\gamma-1}{2}M_\infty^2}{1+\frac{\gamma-1}{2}M_3^2}\right]^{\omega} \tag{26}$$

so that with equation (26) the Reynolds number ratio (eq. (23)) becomes

$$\frac{R_3}{R_\infty}M_\infty^{2\omega}=\frac{p_3/p_\infty}{M_\infty^2}M_3\left[\frac{2}{\gamma-1}\left(1+\frac{\gamma-1}{2}M_3^2\right)\right]^{\omega+1/2} \tag{27}$$

If one desired, this relation could be applied to air also, since the equivalent exponent ω in air is given by (see appendix D, ref. 17):

$$\omega=\frac{3}{2}-\frac{\log\frac{T_3/T_\infty+B/T_\infty}{1+B/T_\infty}}{\log T_3/T_\infty} \tag{28}$$

Values of ω for air are given in figure 20 of reference 16 and were obtained from experimental data and equation (28). If the linear formula for viscosity is used,

$$\frac{\mu_3}{\mu_\infty}=C\frac{T_3}{T_\infty} \tag{29}$$

or, in terms of ω, combining equations (25) and (29) gives

$$C=(T_3/T_\infty)^{\omega-1}$$

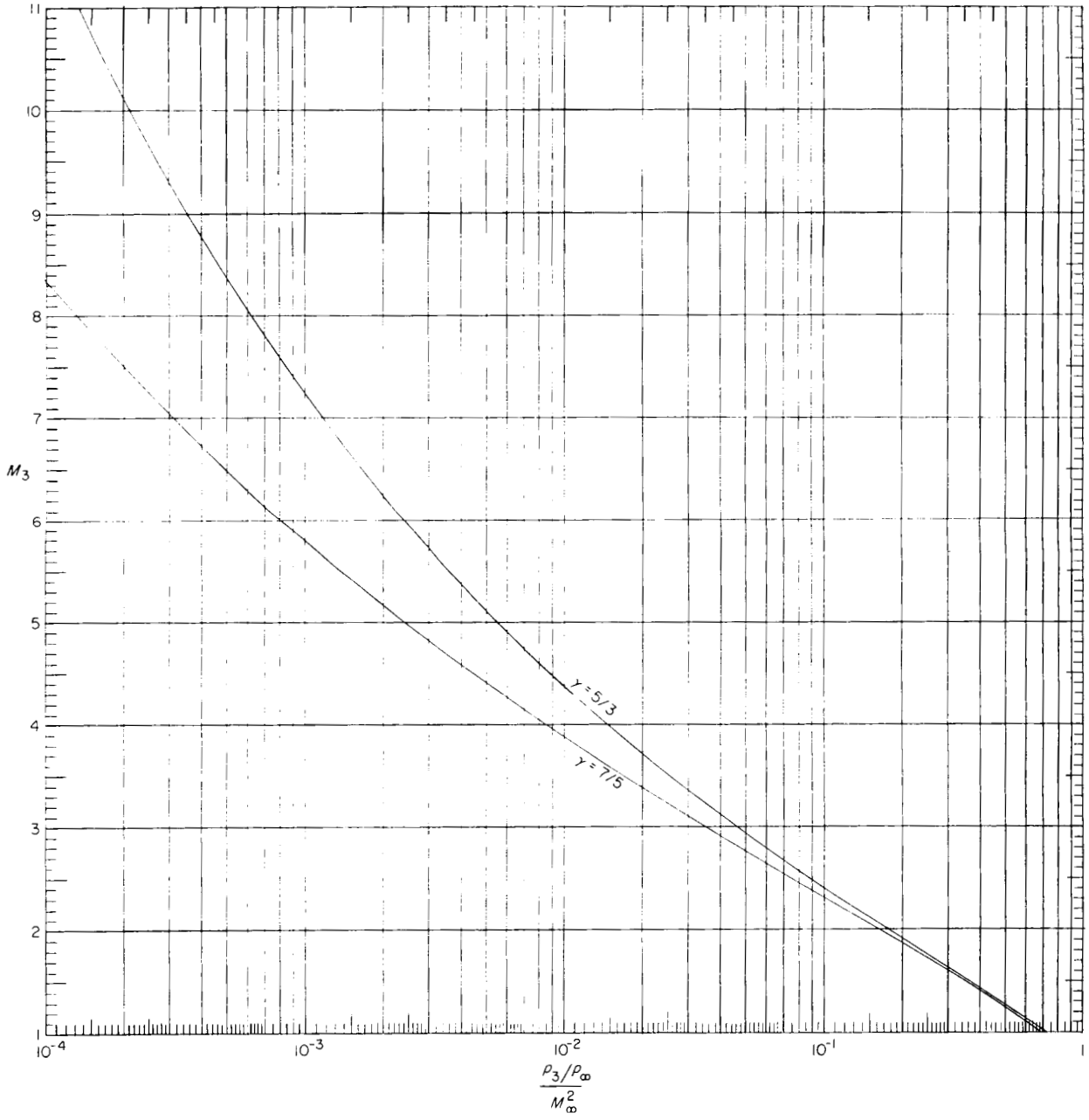

FIGURE 16.—Mach number after expansion from conditions after a normal shock as a function of the hypersonic correlation parameter.

With equation (29) and the same hypersonic approximation as for equation (26), equation (23) may be written as

$$\frac{R_3}{R_\infty} CM_\infty^2 = \frac{p_3/p_\infty}{M_\infty^2} M_3 \left[\frac{2}{\gamma-1}\left(1+\frac{\gamma-1}{2}M_3^2\right)\right]^{3/2} \quad (30)$$

Equation (27) for helium with $\omega=0.65$ and equation (30) for air are shown in figure 17(b).

In terms of the Sutherland formula (eq. (24) with eq. (29)), the coefficient C is

$$C=\sqrt{\frac{T_3}{T_\infty}}\,\frac{1+\frac{B}{T_\infty}}{\frac{T_3}{T_\infty}+\frac{B}{T_\infty}} \quad (31)$$

or to the same approximation as the power-law

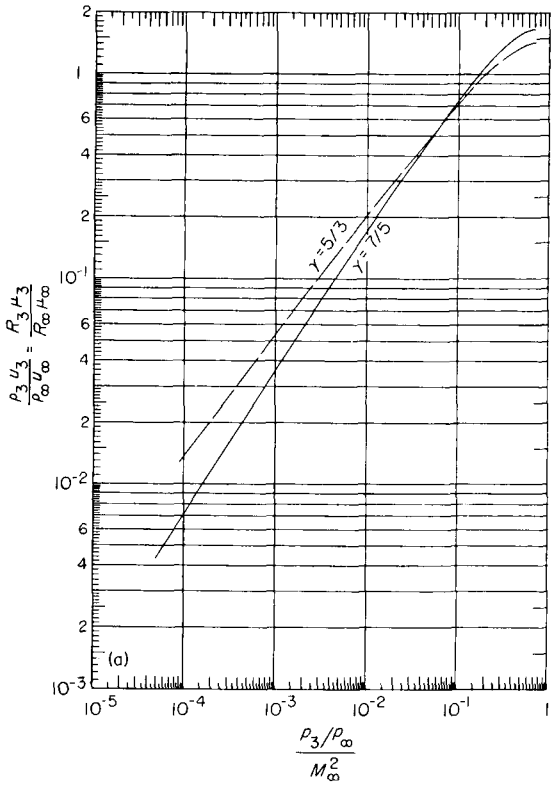

(a) Unit mass-flow ratio.

FIGURE 17.—Reynolds number (or unit mass flow) parameter after expansion from conditions after a normal shock as a function of the hypersonic correlation parameter.

formula (eq. (26))

$$C=\left(\frac{\frac{\gamma-1}{2}M_\infty^2}{1+\frac{\gamma-1}{2}M_3^2}\right)^{1/2}\frac{1+\frac{B}{T_\infty}}{\frac{\frac{\gamma-1}{2}M_\infty^2}{1+\frac{\gamma-1}{2}M_3^2}+\frac{B}{T_\infty}} \tag{32}$$

It must be mentioned here that the accuracy of equations (26), (27), and (32) is not as good as that for M_3 in equation (22) so that calculations based on these equations should be restricted to Mach numbers greater than about 5.

If the local Mach number M_3 and the local Reynolds number R_3 are known, the charts presented in figures 9 to 13 may be used to determine the average turbulent skin-friction coefficient over the plate behind a blunt leading edge. The boundary layer is assumed to be immersed in a high-entropy layer due to a normal shock at the leading edge. Also the case of the sharp-leading-edge flat plate at angle of attack may be evaluated. In the following calculations pressure gradients have been ignored but rather than restrict the calculations to the two-dimensional deflections the computations were carried out in terms of pressure ratio. In the normal-shock case, the local Mach number equation (22) (fig. 16) was used; for air the local Reynolds number equation (23) (fig. 17) was used with equation (24) whereas for helium the local Reynolds number ratio was taken from equation (27). For the sharp-leading-edge case (oblique shock), any of the available charts or tables could be used to obtain local properties. (See refs. 18 to 20, for example, or the well-known oblique-shock equations.)

In order to utilize figures 9 to 13, $C_F/C_{F,i}$ is read as $C_{F,3}/C_{F,i}$, M_∞ as M_3, and R_∞ as R_3. With $C_{F,i}$ evaluated at R_3, $C_{F,3}$ is then found but at local conditions 3. Then in terms of free-stream conditions

$$C_{F,3,\infty}=C_{F,3}\frac{p_3}{p_\infty}\left(\frac{M_3}{M_\infty}\right)^2 \tag{33}$$

An example of these calculations is shown in figure 18. Here the pressure over the plate is assumed to be equal to the undisturbed free-stream pressure ($p/p_\infty=1$ and $R_{\infty,x}=10^8$). The skin friction for the blunt case is shown with respect to that for the sharp case at the equivalent wall temperature. A considerable decrease in skin friction due to the normal shock at the leading edge is shown. This decrease in skin friction is larger for air than it is for helium. The effect of undisturbed free-stream temperature level on the air results is negligible for all practical purposes. The greatest effect of the blunt leading edge is found at the lower Mach numbers, and the effect of leading-edge blunting decreases as the Mach number increases and is more pronounced at $T_w=0$ than for the insulated-plate case.

An obvious extension of these calculations is to the case where the surface pressure ratio is other than unity. The approach in this case is the same except for the changed surface pressure which is again constant over the plate. The effect of pressure level on the average skin-friction coefficient in turbulent flow is shown in figure 19. Values of $\gamma=5/3$ and $7/5$ were used, as for previous

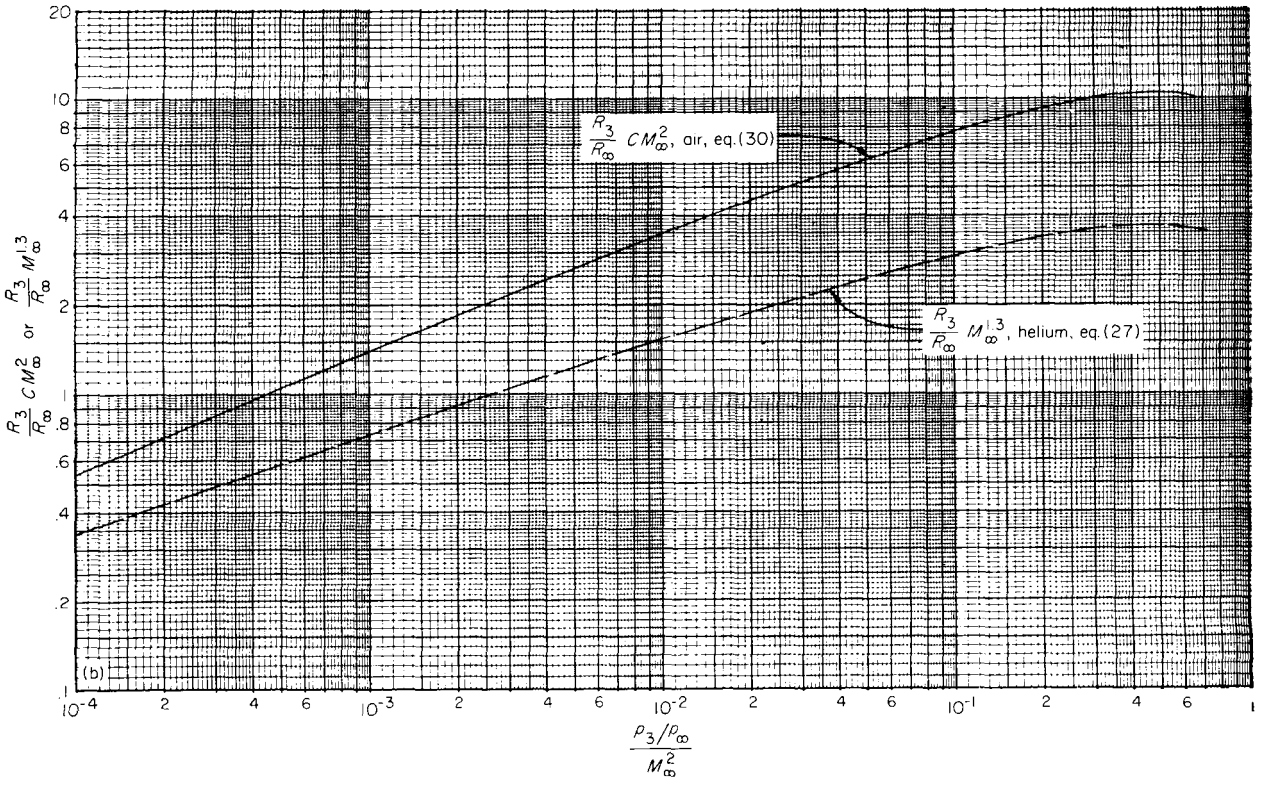

(b) Reynolds number parameter.

FIGURE 17.—Concluded.

calculations, and wall temperatures corresponding to the insulated plate and absolute zero were chosen at a free-stream Reynolds number of 10^5.

The results indicate that for the oblique-shock (sharp-leading-edge) case the skin friction varies as the pressure ratio to about the 0.77 power and for the normal-shock case, to about the 0.68 power at the lower pressure ratios for each Mach number. However, the skin friction eventually reaches a peak and then decreases with further increases in pressure. The maximum skin friction occurs at about the value of pressure ratio over the plate where $p/p_\infty \approx M_\infty^2/2$. The decrease in skin friction due to the normal shock is manifested at all pressure ratios but the effect of blunting on skin friction increases as the pressure ratio increases as indicated by the powers for the skin-friction—pressure-ratio dependence cited previously. For the oblique-shock (sharp-leading-edge) case the curves of the skin-friction ratio for the same Mach number are very much the same for the different wall temperatures and ratios of specific heat investigated. The effect of undisturbed free-stream temperature was investigated and was found to be negligible at all pressure ratios (as for the case where the pressure ratio is unity presented in fig. 18).

It is well to point out before leaving this effect of pressure ratio that neither boundary-layer-displacement effects nor the pressures induced by a blunt leading edge have been considered. Boundary-layer self-induced effects in hypersonic flow have been extensively investigated in laminar flow (for example, see refs. 17 and 21) but not to any great extent in turbulent flow. The boundary-layer displacement effect in turbulent flow has been considered by Monaghan. (See ref. 5.) His calculations indicated that the pressure gradient dp/dx was smaller in turbulent flow than in laminar flow; thus, the main effect may be a change in overall pressure level on the plate. Based on the calculations presented in figure 19, such an increase in pressure could have a significant effect on the skin friction at the lower pressure ratios (corresponding to low angles of attack). The blunt leading edge in hypersonic flow can

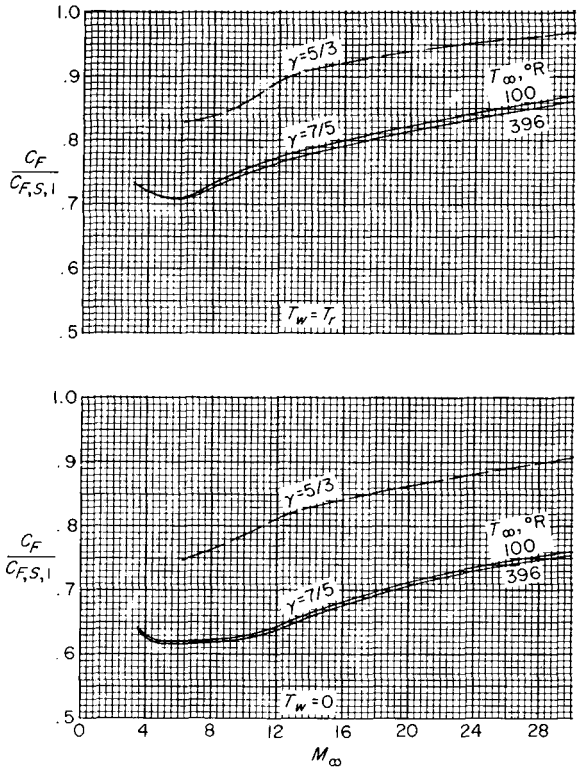

FIGURE 18.—Ratio of average skin friction on blunt-leading-edge plate to skin friction on sharp-leading-edge plate as a function of Mach number. Pressure on both sharp- and blunt-leading-edge plates equal to undisturbed free-stream pressure. $R_{\infty,x}=10^8$; air and helium.

cause large increases in pressure over extensive distances on a plate. (See, for example, ref. 22.) The bluntness-induced effects, however, will be considerably reduced if the leading edge is swept. (See ref. 21.) Because of the pressures induced by leading-edge blunting, the decrease in skin friction due to leading-edge blunting at a given pressure ratio (figs. 18 and 19) will probably not be realized in the practical case, at least, at low angles of attack.

APPLICATION OF RESULTS TO CONE AND TAPERED PLATE

AVERAGE TURBULENT SKIN FRICTION FOR A CONE AT ZERO ANGLE OF ATTACK

The differential shearing force on a cone whose geometry is shown in the following sketch is

$$d\tau_c=2\pi r C_{f,c} q dx \tag{34}$$

or expressed in integral form and normalized

$$C_{F,c}=\frac{\tau_c}{qS}=\frac{2}{l^2}\int_0^l C_{f,c} x dx \tag{35}$$

where S is the surface area of the cone.

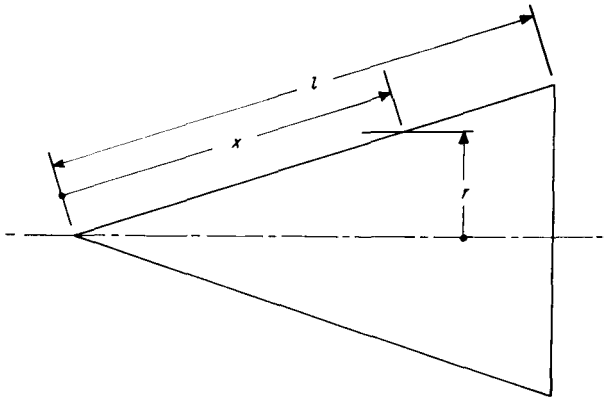

By utilizing Van Driest's rule for the local turbulent skin friction on a cone (ref. 23) with the power law, the local skin-friction coefficient is given by

$$C_{f,c}=b\left(\frac{R_x}{2}\right)^n \tag{36}$$

Substitution of equation (36) into equation (35) and integration yield

$$C_{F,c}=\frac{2^{1-n}}{2+n} bR_l^n \tag{37}$$

For a flat plate the differential shearing force is

$$d\tau_{fp}=C_{f,fp} q dx \tag{38}$$

or when expressed in integral form and normalized

$$C_{F,fp}=\frac{\tau_{fp}}{ql}=\frac{1}{l}\int_0^l C_f dx \tag{39}$$

In this case the local skin-friction coefficient is given by

$$C_{f,fp}=bR_x^n \tag{40}$$

and substitution of equation (40) into equation (39) and integration yield

$$C_{F,fp}=\frac{bR_l^n}{1+n} \tag{41}$$

where $b/(1+n)$ is the same as the coefficient a in equation (17).

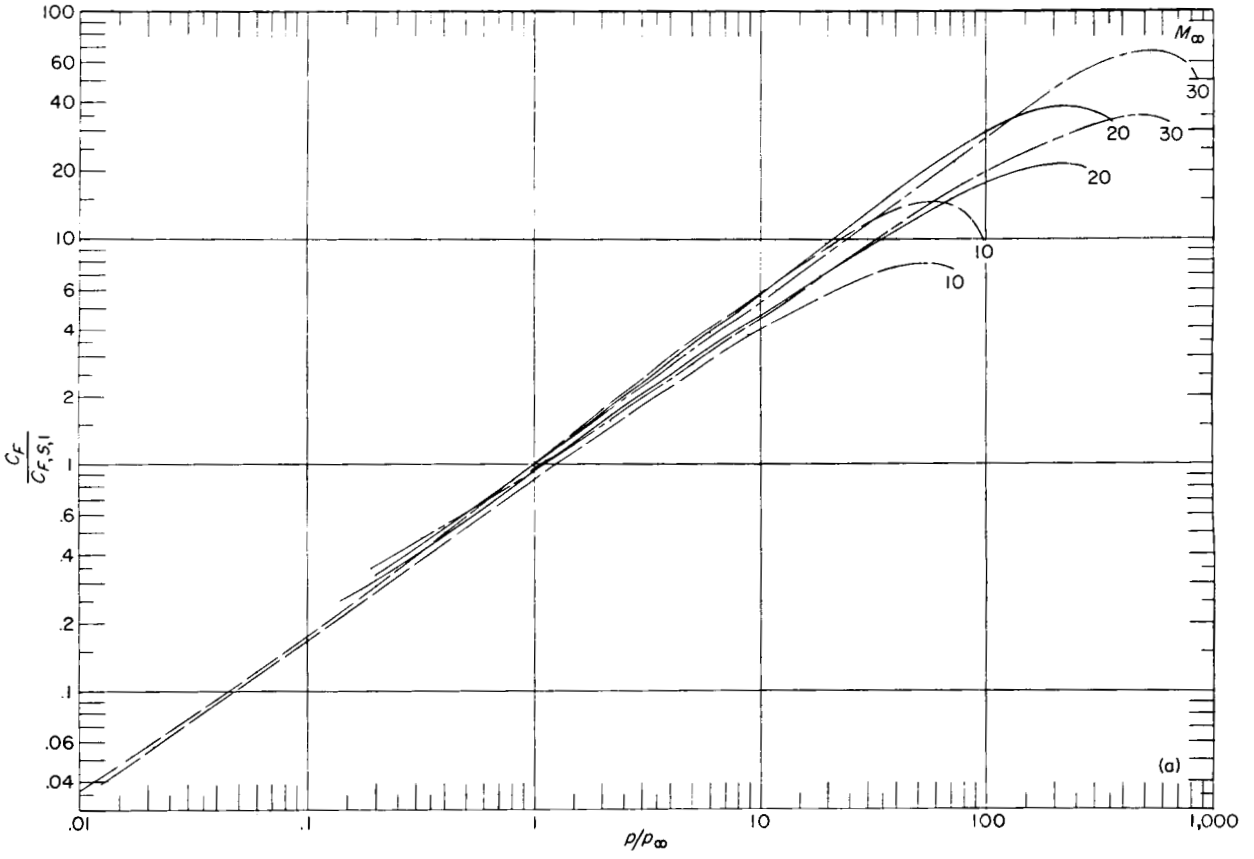

(a) $\gamma=5/3$ (helium); $T_w=T_r$.

FIGURE 19.—Effect of pressure level on average skin friction on one side of sharp- and blunt-leading-edge flat plates. At a given Mach number the upper curve represents the sharp-leading-edge case; the lower curve, the blunt-leading-edge case. $R_{\infty,x}=10^8$.

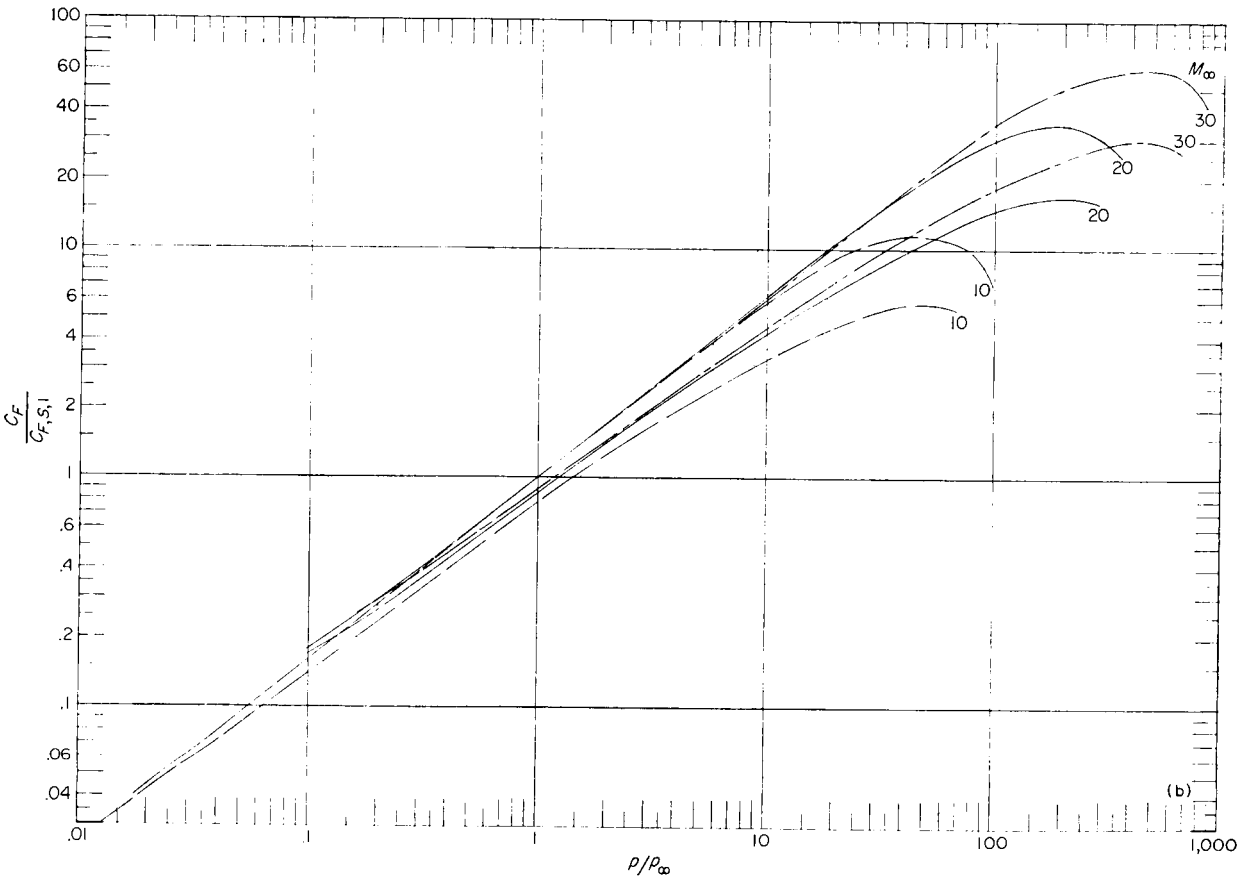

(b) $\gamma=5/3$ (helium); $T_w=0°$ absolute.

FIGURE 19.—Continued.

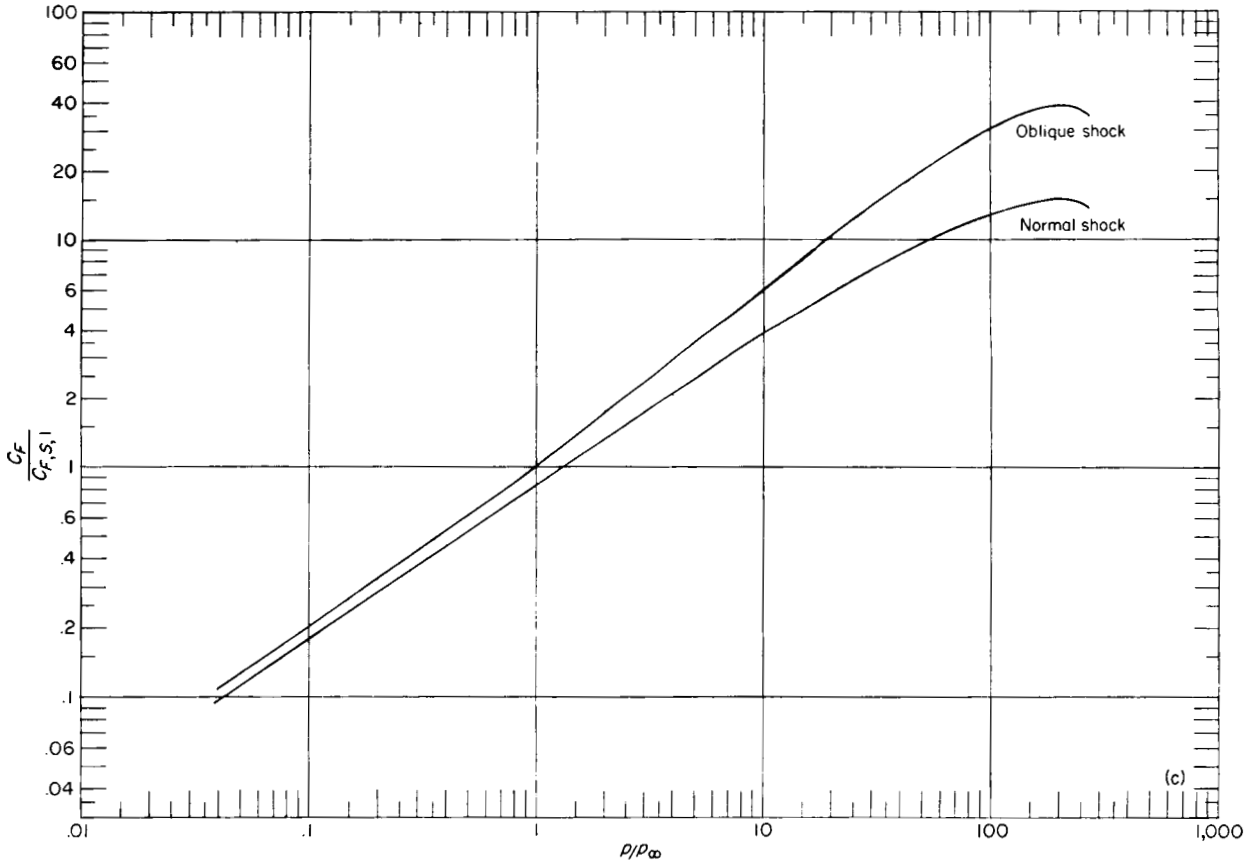

(c) $\gamma=7/5$ (air); $T_w=T_r$; $M_\infty=20$.

FIGURE 19.—Continued.

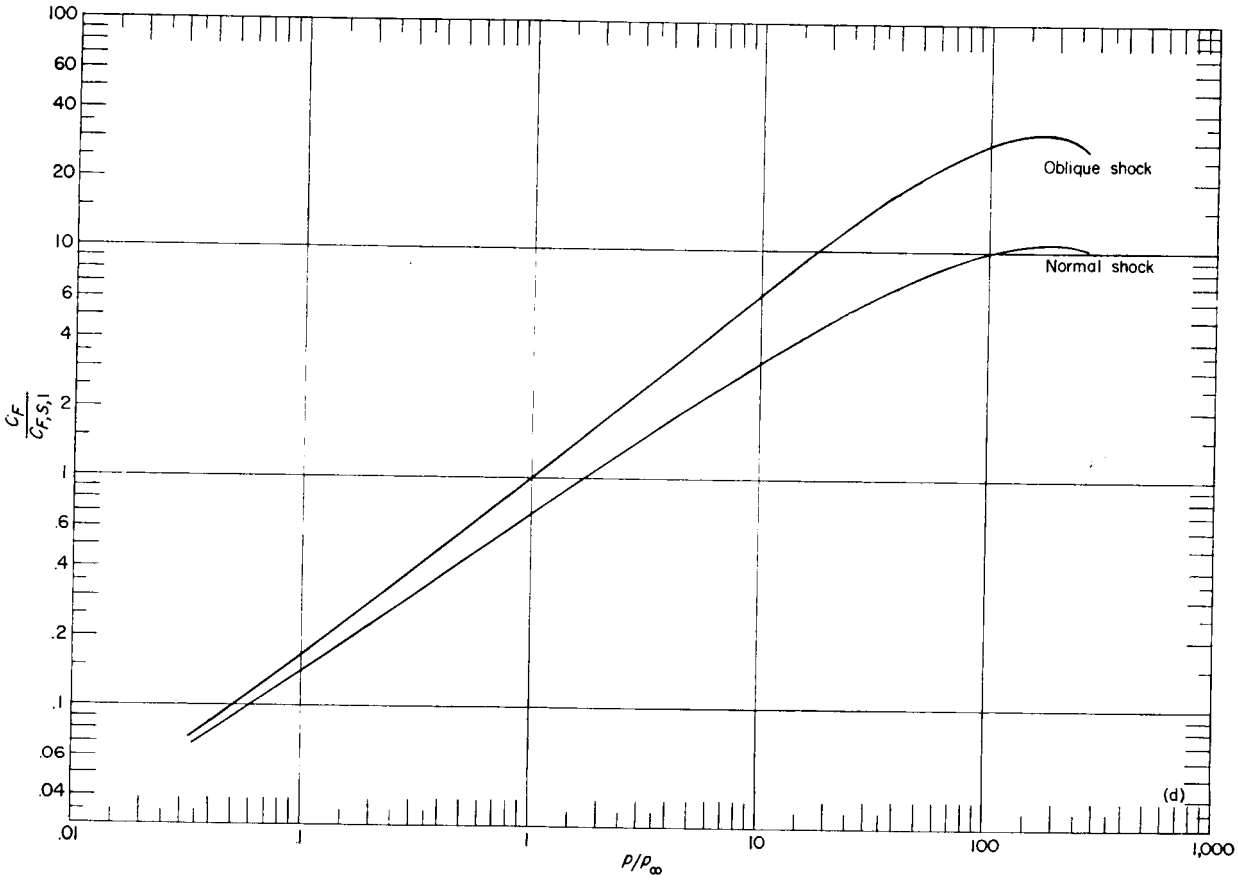

(d) $\gamma=7/5$ (air); $T_w=0°$ absolute; $M_\infty=20$.

FIGURE 19.—Concluded.

The ratio of the average skin-friction coefficient on a cone to that on a flat plate for the same Reynolds number based on length and the same local conditions is thus given by the ratio of equation (37) to equation (41)

$$\frac{C_{F,c}}{C_{F,fp}}=2^{1-n}\frac{1+n}{2+n} \tag{42}$$

This result is plotted at the top of figure 20 and shows that for all practical purposes the average turbulent skin friction on a cone is the same as that for a flat plate essentially independent of the exponent in the power law for turbulent skin friction. This result may be compared with that from laminar flow where

$$\frac{C_{F,c}}{C_{F,fp}}=\frac{2}{\sqrt{3}}\approx 1.155.$$

AVERAGE SKIN FRICTION FOR A TAPERED PLATE

It can be shown from the results of appendix D of reference 17 that, if streamwise flow on the surface is assumed and the skin friction along any longitudinal element of the triangular planform plate is assumed to be given by a power law (eq. (17)), the ratio of the skin-friction coefficient on a triangular plate to that on a flat plate (local conditions the same) is given by

$$\frac{C_{f,\lambda=0}}{C_{F,fp}}=\frac{2}{2+n} \tag{43}$$

where the Reynolds number based on the root chord of the triangular plate is assumed to be the same as that based on the chord of the flat plate and the pressure is constant over the plates. Whereas the previous development for a cone is only applicable to turbulent flow because of the limitation imposed by equation (36), equation (43) is applicable to laminar flow as well. With an approach similar to that in reference 17, a more general expression for skin friction may be obtained which applies to any wing of tapered planform with tips cut off parallel to the stream direction; that is,

$$\frac{C_{F,\lambda}}{C_{F,fp}}=\frac{1-\lambda^{2+n}}{1-\lambda^2}\,\frac{2}{2+n} \tag{44}$$

where the Reynolds number based on the root chord of the tapered planform plate is assumed to be the same as that based on the chord of the rectangular flat plate. A plot of equation (44) is shown at the bottom of figure 20. The greatest increase in skin-friction coefficient for a tapered plate is found in laminar flow ($n^{-1}=-2$). From figure 15 note that, for turbulent flow, values of n^{-1} from about -3 to perhaps -7 or -8 are of interest. Over this range of n^{-1} the increase in skin-friction coefficient for a triangular plate ($\lambda=0$) is not large (an increase by a factor of about 1.2 down to 1.07) so that an average value of, say, 1.1 for the skin-friction coefficient ratio should suffice over a considerable range of Reynolds number. Similarly, average values for practical use can be arrived at from figure 20 for other taper ratios.

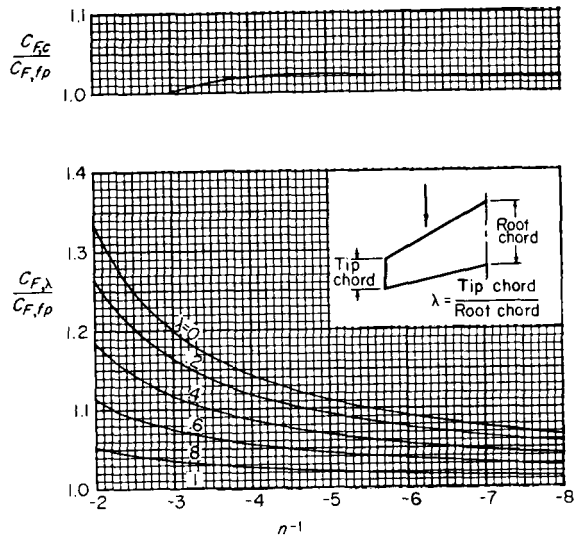

FIGURE 20.—Ratio of average turbulent skin-friction coefficient on a cone and a tapered plate to that on a flat plate where the Reynolds number is the same based on length or root chord, as the case may be, as a function of the inverse of the exponent in the power law for skin friction.

CONCLUDING REMARKS

Calculations have been carried out for a perfect-gas flow to show the effect of a wide range of parameters on the average skin friction on a flat plate in turbulent flow by the reference-temperature method (however, to some extent laminar flow was also treated). Some of the variables were Mach number, Reynolds number, and wall and free-stream temperature level for ratios of

specific heats of 7/5 and 5/3. The effect of the blunt leading edge was calculated by assuming the turbulent boundary layer to be growing in the reexpanded flow behind a normal shock at various free-stream Mach numbers. Analogous to angle of attack, the pressure level on the plate was varied over a wide range to show the effect on skin friction for the sharp and the blunt leading edges. Relations which allow the results to be applied to cones and wings of tapered planform were shown.

LANGLEY RESEARCH CENTER,
NATIONAL AERONAUTICS AND SPACE ADMINISTRATION,
LANGLEY STATION, HAMPTON, VA., *August 2, 1961.*

REFERENCES

1. Rubesin, M. W., and Johnson, H. A.: A Critical Review of Skin-Friction and Heat-Transfer Solutions of the Laminar Boundary Layer of a Flat Plate. Trans. A.S.M.E., vol. 71, no. 4, May 1949, pp. 383–388.
2. Fischer, W. W., and Norris, R. H.: Supersonic Convective Heat-Transfer Correlation From Skin-Temperature Measurements on a V–2 Rocket in Flight. Trans. A.S.M.E., vol. 71, no. 5, July 1949, pp. 457–469.
3. Young, A. D.: Skin Friction in the Laminar Boundary Layer in Compressible Flow. Rep. No. 20, The College of Aeronautics, Cranfield (British), July 1948.
4. Monaghan, R. J.: An Approximate Solution of the Compressible Laminar Boundary Layer on a Flat Plate. R. & M. No. 2760, British A.R.C., 1956.
5. Monaghan, R. J.: On the Behaviour of Boundary Layers at Supersonic Speeds. Fifth International Aeronautical Conference (Los Angeles, Calif., June 20–23, 1955), Inst. Aero. Sci., Inc., 1955, pp. 277–315.
6. Zahm, A. F.: Fluid Friction on Smooth Planes. Jour. Aero. Sci., vol. 4, no. 12, Oct. 1937, pp. 504–506.
7. Locke, F. W. S., Jr.: Recommended Definition of Turbulent Friction in Incompressible Fluids. NAVAER DR Rep. No. 1415, Bur. Aero., June 1952.
8. Smith, Donald W., and Walker, John H.: Skin-Friction Measurements in Incompressible Flow. NASA TR R–26, 1959. (Supersedes NACA TN 4231.)
9. Sivells, James C., and Payne, Robert G.: A Method of Calculating Turbulent-Boundary-Layer Growth at Hypersonic Mach Numbers. AEDC-TR-59–3, ASTIA Doc. No. AD–208774, Arnold Eng. Dev. Center, Mar. 1959.
10. Van Driest, E. R.: Investigation of Laminar Boundary Layer in Compressible Fluids Using the Crocco Method. NACA TN 2597, 1952.
11. Chapman, Dean R., and Kester, Robert H.: Turbulent Boundary-Layer and Skin-Friction Measurements in Axial Flow Along Cylinders at Mach Numbers Between 0.5 and 3.6. NACA TN 3097, 1954.
12. Matting, Fred W., Chapman, Dean R., Nyholm, Jack R., and Thomas, Andrew G.: Turbulent Skin Friction at High Mach Numbers and Reynolds Numbers in Air and Helium. NASA TR R–82, 1961.
13. Schultz-Grunow, F.: New Frictional Resistance Law for Smooth Plates. NACA TM 986, 1941.
14. Coles, Donald: Measurements in the Boundary Layer on a Smooth Flat Plate in Supersonic Flow. III. Measurements in a Flat-Plate Boundary Layer at the Jet Propulsion Laboratory. Rep. No. 20–71 (Contract No. DA–04–495–Ord 18), Jet Propulsion Lab., C.I.T., June 1, 1953.
15. Hill, F. K.: Boundary-Layer Measurements in Hypersonic Flow. Jour. Aero. Sci., vol. 23, no. 1, Jan. 1956, pp. 35–42.
16. Love, Eugene S., Henderson, Arthur, Jr., and Bertram, Mitchel H.: Some Aspects of Air-Helium Simulation and Hypersonic Approximations. NASA TN D–49, 1959.
17. Bertram, Mitchel H.: Boundary-Layer Displacement Effects in Air at Mach Numbers of 6.8 and 9.6. NASA TR R–22, 1959. (Supersedes NACA TN 4133.)
18. Ames Research Staff: Equations, Tables, and Charts for Compressible Flow. NACA Rep. 1135, 1953. (Supersedes NACA TN 1428.)
19. Mueller, James N.: Equations, Tables, and Figures for Use in the Analysis of Helium Flow at Supersonic and Hypersonic Speeds. NACA TN 4063, 1957.
20. Henderson, Arthur, Jr., and Braswell, Dorothy O.: Charts for Conical and Two-Dimensional Oblique-Shock Flow Parameters in Helium at Mach Numbers From About 1 to 100. NASA TN D–819, 1961.
21. Bertram, Mitchel H., and Henderson, Arthur, Jr.: Effects of Boundary-Layer Displacement and Leading-Edge Bluntness on Pressure Distribution, Skin Friction, and Heat Transfer of Bodies at Hypersonic Speeds. NACA TN 4301, 1958.
22. Baradell, Donald L., and Bertram, Mitchel H.: The Blunt Plate in Hypersonic Flow. NASA TN D–408, 1960.
23. Van Driest, E. R.: Turbulent Boundary Layer on a Cone in a Supersonic Flow at Zero Angle of Attack. Jour. Aero. Sci., vol. 19, no. 1, Jan. 1952, pp. 55–57, 72.

U.S. GOVERNMENT PRINTING OFFICE: 1963